A Chaikin-based variant of Lane-Riesenfeld algorithm and its non-tensor product extension

A Chaikin-based variant of Lane-Riesenfeld algorithm and its non-tensor product extension

Lucia Romani[a,*]

[a]*Dipartimento di Matematica e Applicazioni, Università di Milano-Bicocca, Via R. Cozzi 55, 20125 Milano, Italy*

Abstract

In this work we present a parameter-dependent Refine-and-Smooth (*RS*) subdivision algorithm where the refine stage R consists in the application of a perturbation of Chaikin's/Doo-Sabin's vertex split, while each smoothing stage S performs averages of adjacent vertices like in the Lane-Riesenfeld algorithm [19]. This constructive approach provides a unifying framework for univariate/bivariate primal and dual subdivision schemes with tension parameter and allows us to show that several existing subdivision algorithms, proposed in the literature via isolated constructions, can be obtained as specific instances of the proposed strategy. Moreover, this novel approach provides an intuitive theoretical tool for the derivation of new non-tensor product subdivision schemes with bivariate cubic precision, which appear as the natural extension of the univariate family presented in [18].

Keywords: Subdivision; Refine-and-Smooth; Tension parameter; Non-tensor product; Bivariate cubic precision

1. Introduction

The beginning of subdivision for surface modelling goes back to 1978 when the generalizations for bi-quadratic and bi-cubic B-spline surfaces to quadrilateral meshes of arbitrary topology were published simultaneously by Catmull and Clark [2] and by Doo and Sabin [12]. Then, in 1980 Lane and Riesenfeld [19] provided a unified framework to represent for all $n \in \mathbb{N}$, degree-$(n+1)$ uniform B-spline curves and their tensor product extensions via a subdivision process where each subdivision step consists in applying one refine stage (aimed at doubling the number of given vertices) followed by n smoothing stages which modify the vertices position but not their number. In formulas, each subdivision step consists in the application of the subdivision operator S^nR, where R and S denote the refine and smoothing operators, respectively. All processes of this kind are named *Refine-and-Smooth (RS) algorithms*, and the one proposed by Lane and Riesenfeld is certainly the simplest example that can be found in the literature since the refine operator R is given by the subdivision scheme for linear splines, while each smoothing operator S averages adjacent vertices in the current data set. Twenty years later, Stam [23] on the one side and Zorin and Schröder [24] on the other side, proposed independently a generalization of the Lane-Riesenfeld algorithm to arbitrary meshes, and showed that Doo-Sabin and Catmull-Clark schemes are nothing but the first two members of a family of surface subdivision schemes (also known in the literature as the family of *midpoint subdivision schemes*), which generalizes uniform tensor product B-spline surfaces of any bi-degree to quadrilateral meshes of arbitrary topology. The n-th member ($n \in \mathbb{N}$) of such a family is shown to produce a C^n continuous limit surface, except at extraordinary vertices (i.e., vertices of valence other than 4) where the continuity is always C^1. Exploiting Reif's criterion in [22], Zorin and Schröder were able to show the C^1-smoothness of the limit surfaces at extraordinary vertices for the first 8 family members. A general analysis tool to prove C^1 smoothness for any $n \geq 1$ appeared only with the publication of [21]. Since the family of midpoint subdivision schemes relies on a smoothing operator S performing midpoint averages (exactly as the standard Lane-Riesenfeld algorithm), it is made of an alternation of *dual*/*primal* members, corresponding to the application of an odd/even number n of smoothing stages, respectively. Indeed, when an odd number of

*Corresponding author
Email address: lucia.romani@unimib.it (Lucia Romani)

smoothing stages is applied, the resulting subdivision scheme is featured by rules performing a vertex split; in contrast, the univariate/bivariate scheme obtained by the operator S^nR with n even, recursively subdivides a given mesh via an edge/face split operation.

The goal of this work is to present a new constructive approach to design univariate and bivariate families of alternating primal/dual subdivision schemes with tension parameter in a unified framework. The approach is based on a *RS* subdivision algorithm where the refine stage consists in the application of a perturbation of the standard subdivision scheme for quadratic splines, while each smoothing stage usually performs averages of adjacent vertices. Therefore, in the univariate context, the refine stage is based on a parameter-dependent variant of Chaikin's corner cutting algorithm [3], whereas in the bivariate context on an analogous modification of Doo-Sabin's algorithm for polyhedral meshes with arbitrary faces [12]. Considering n smoothing stages as in Lane-Riesenfeld algorithm, this novel *RS* algorithm allows us to derive families of curve and surface subdivision schemes whose structure and properties are very similar to those of the B-spline schemes. In fact, the members of each family are also enumerated by n, and higher values of n give schemes with wider masks and support, higher continuity and higher degree of polynomial generation. The main difference is that, when suitably setting the tension parameter, all schemes from the new family are able to reproduce cubic polynomials, whereas the B-spline schemes have only linear precision. Moreover, exactly as B-spline schemes, the new schemes can be conveniently implemented using repeated local operations that only involve direct neighbors of the newly inserted or updated vertices. In the univariate context, this new construction provides a whole family of tension-controlled curve subdivision schemes, whose first two members coincide with the well-known interpolatory 4-point and dual 4-point schemes with tension parameter, presented via isolated constructions in [14] and [16], respectively. In addition, the new family contains the family of subdivision schemes with cubic precision proposed in [18], as a special subfamily. The generalization of the tension-controlled univariate family to quadrilateral meshes of arbitrary topology yields a family of non-tensor product schemes with tension parameter. If considering a specific setting of the free parameter, we show that the new family results in a subfamily of non-tensor product subdivision schemes reproducing bivariate cubic polynomials. The first member of the resulting subfamily (corresponding to $n = 1$ smoothing stages) coincides with the interpolatory subdivision scheme for quadrilateral meshes with arbitrary topology already presented in [10], but not yet analyzed. Differently, the second family member obtained by means of $n = 2$ smoothing stages, is a completely new dual approximating subdivision scheme for quadrilateral meshes of arbitrary topology, whose properties are deeply investigated.

The content of this paper is organized in six sections. Section 2 provides the background on d-variate subdivision schemes and reminds some existing results related to the Refine-and-Smooth mechanism. In Section 3 a new family of Refine-and-Smooth (*RS*) univariate subdivision schemes with tension parameter is introduced and its main properties are analyzed. Section 4 extends the idea presented in Section 3 to design a new family of tension-controlled *RS* subdivision schemes for quadrilateral meshes of arbitrary topology. In Sections 5 and 6 special attention is addressed to the description and the analysis of the first two family members resulting from the proposed construction. Conclusions are drawn in Section 7.

2. Background

We start this section by reminding some known facts about scalar d-variate subdivision schemes.

2.1. Basic notions

A binary scalar d-variate ($d = 1, 2$) subdivision scheme is univocally identified by a scalar finitely supported sequence $\mathbf{a} = \{\mathrm{a}_\mathbf{i} \in \mathbb{R}, \mathbf{i} \in \mathbb{Z}^d\}$ called *mask*. For all subdivision levels $k \in \mathbb{N}_0 = \mathbb{N} \cup \{0\}$, the operator $\mathcal{S}_\mathbf{a}$ mapping the data sequence $\mathbf{P}^{(k)} = \{\mathbf{p}_\mathbf{i}^{(k)} \in \mathbb{R}^3, \mathbf{i} \in \mathbb{Z}^d\}$ into the data sequence $\mathbf{P}^{(k+1)} = \mathcal{S}_\mathbf{a}\mathbf{P}^{(k)}$ with

$$(\mathcal{S}_\mathbf{a}\mathbf{P}^{(k)})_\mathbf{i} = \sum_{\mathbf{j}\in\mathbb{Z}^d} \mathrm{a}_{\mathbf{i}-2\mathbf{j}}\, \mathbf{p}_\mathbf{j}^{(k)}, \qquad \mathbf{i} \in \mathbb{Z}^d$$

is called *subdivision operator*. The iterative algorithm based on the repeated application of the subdivision operator $\mathcal{S}_\mathbf{a}$ starting from the initial data $\mathbf{P}^{(0)}$ is termed *subdivision scheme* and is also denoted by $\mathcal{S}_\mathbf{a}$. If convergent, this iterative algorithm produces in the limit a parametric curve/surface with each component being a d-variate function

which is the limit of $\mathcal{S}_{\mathbf{a}}$ applied to the corresponding component of the initial data. Therefore, in order to study the convergence of a scalar d-variate subdivision scheme $\mathcal{S}_{\mathbf{a}}$ it is sufficient to focus on the functional setting and construct the function $\mathcal{F}^{(k)} : \mathbb{R}^d \to \mathbb{R}$ as the piecewise linear interpolant to the k-level data $\{(2^{-k}\mathbf{i}, f_{\mathbf{i}}^{(k)}) : \mathbf{i} \in \mathbb{Z}^d\}$, with $F^{(k)} = \{f_{\mathbf{i}}^{(k)} \in \mathbb{R} : \mathbf{i} \in \mathbb{Z}^d\}$ the set of values obtained as $F^{(k)} = \mathcal{S}_{\mathbf{a}}^k F^{(0)}$, and $F^{(0)}$ the sequence of initial values made of the selected component of the data sequence $\mathbf{P}^{(0)}$. The subdivision scheme is defined to be *convergent* if for any bounded initial data $F^{(0)}$ the sequence $\{\mathcal{F}^{(k)}(\boldsymbol{x}) : k \in \mathbb{N}_0\}$ is a Cauchy sequence in the norm $\sup\{\mathcal{F}^{(k)}(\boldsymbol{x}) : \boldsymbol{x} \in \mathbb{R}^d\}$, and the limit is non-zero for the data $\boldsymbol{\delta} = \{\delta_{\mathbf{0}} = 1, \delta_{\mathbf{i}} = 0 \text{ for } \mathbf{i} \neq \mathbf{0}\}$. The limit $\mathcal{S}_{\mathbf{a}}^{\infty}\boldsymbol{\delta}$ is called the *basic limit function* (BLF for short) of the subdivision scheme. A well-established tool for analyzing the smoothness properties of the basic limit function (and hence of the associated subdivision scheme) is given by the so-called *mask symbol* [15], i.e. the Laurent polynomial

$$a(\boldsymbol{z}) = \sum_{\mathbf{i}\in\mathbb{Z}^d} \mathrm{a}_{\mathbf{i}} \boldsymbol{z}^{\mathbf{i}}, \qquad \boldsymbol{z} = (z_1, ..., z_d) \in (\mathbb{C}\backslash\{0\})^d$$

constructed via the mask entries. Denoting by $\Xi = \{0, 1\}^d$ the set of representatives of $\mathbb{Z}^d/2\mathbb{Z}^d$ containing $\mathbf{0} = (0, 0, ..., 0)$, the 2^d *submasks* and the associated *subsymbols* $a_\xi(\boldsymbol{z})$ are respectively defined by $\{\mathrm{a}_{\xi+2\mathbf{i}},\ \mathbf{i} \in \mathbb{Z}^d\}$ and

$$a_\xi(\boldsymbol{z}) = \sum_{\mathbf{i}\in\mathbb{Z}^d} \mathrm{a}_{\xi+2\mathbf{i}}\, \boldsymbol{z}^{\mathbf{i}} \qquad \text{with} \quad \xi \in \Xi.$$

Therefore the mask symbol $a(\boldsymbol{z})$ can be written in terms of its subsymbols as $a(\boldsymbol{z}) = \sum_{\xi\in\Xi} \boldsymbol{z}^{\xi} a_\xi(\boldsymbol{z}^2)$.

Remark 1. *Note that, for simplicity of notation, in the univariate case ($d = 1$), the two subsymbols $a_0(z)$ and $a_1(z)$ are usually labeled as $a_{even}(z)$ and $a_{odd}(z)$, respectively.*

For the work done in this paper, it is also important to remind that, when studying the convergence properties of a subdivision scheme, the choice of the parameter values $\mathbf{t}_{\mathbf{i}}^{(k)}$ to which the k-level values $f_{\mathbf{i}}^{(k)} \in \mathbb{R}$, $\mathbf{i} \in \mathbb{Z}^d$, are associated to construct the piecewise linear interpolant $\mathcal{F}^{(k)}(\boldsymbol{x})$, is totally irrelevant and thus usually set to $\mathbf{t}_{\mathbf{i}}^{(k)} = \frac{\mathbf{i}}{2^k}$. Differently, when checking the capability of a subdivision scheme to reproduce polynomials, the choice of the parameter values $\mathbf{t}_{\mathbf{i}}^{(k)}$ becomes crucial and the standard setting $\mathbf{t}_{\mathbf{i}}^{(k)} = \frac{\mathbf{i}}{2^k}$, $\mathbf{i} \in \mathbb{Z}^d$, is not always optimal. Thus, a more general expression depending on a *shift parameter* $\boldsymbol{\tau} \in \mathbb{R}^d$ as follows

$$\mathbf{t}_{\mathbf{i}}^{(k)} = \frac{\mathbf{i} + \boldsymbol{\tau}}{2^k}, \qquad \mathbf{i} \in \mathbb{Z}^d,\ k \in \mathbb{N}_0 \tag{2.1}$$

has been proven to be more convenient [4, 6, 7, 8]. The correct choice of $\boldsymbol{\tau}$ is given by

$$\boldsymbol{\tau} = \frac{(D^{\boldsymbol{\epsilon}_1} a(\mathbf{1}), ..., D^{\boldsymbol{\epsilon}_d} a(\mathbf{1}))}{2^d}, \tag{2.2}$$

where $\boldsymbol{\epsilon}_j$ denotes the j-th unit vector of $\mathbb{R}^d$ (see [4, Proposition 2.3]). For instance, in the univariate case ($d = 1$) we have $\tau = \frac{D^{(1)}a(1)}{2}$ (see [7, Theorem 3.1]) and in the bivariate case ($d = 2$), $\boldsymbol{\tau} \equiv (\tau_1, \tau_2) = \frac{(D^{(1,0)}a(1,1), D^{(0,1)}a(1,1))}{4}$. If (2.2) provides $\boldsymbol{\tau} = (0, ..., 0)$ then $\mathbf{t}_{\mathbf{i}}^{(k)} = \frac{\mathbf{i}}{2^k}$ and the parametrization is called either *standard* or *primal*. If (2.2) provides $\boldsymbol{\tau} = (\frac{1}{2}, ..., \frac{1}{2})$ then $\mathbf{t}_{\mathbf{i}}^{(k)} = \frac{\mathbf{i}+(\frac{1}{2},...,\frac{1}{2})}{2^k}$ and the parametrization is called *dual* (see [4, 6, 7, 8]).

Let Π^d denote the space of all d-variate polynomials with real coefficients and Π_g^d the subspace of polynomials of total degree at most g. The following results summarize the algebraic conditions that the subdivision symbol of a convergent and *non-singular* d-variate subdivision scheme $\mathcal{S}_{\mathbf{a}}$ (i.e., such that $\mathcal{S}_{\mathbf{a}}^{\infty}F^{(0)} = \mathbf{0}$ if and only if $F^{(0)} = \mathbf{0}$) has to satisfy in order to generate or reproduce Π_g^d. We remind that the generation degree of a subdivision scheme is the maximum degree of polynomials that can potentially be generated by the scheme, provided that the initial data is chosen correctly. Obviously, it is not less than the reproduction degree. For the precise definition of polynomial generation and reproduction the reader can consult [4, 7, 13].

Proposition 2.1. *[7, 8] A univariate subdivision scheme $\mathcal{S}_{\mathbf{a}}$*

(i) generates Π_g^1 *if and only if*

$$a(1) = 2, \;\; a(-1) = 0 \quad \textit{and} \quad D^{(j)}a(-1) = 0, \;\; j = 1, ..., g;$$

(ii) reproduces Π_g^1 *with respect to the parametrization* $\{t_i^{(k)} = \frac{i+\tau}{2^k}\}_{i\in\mathbb{Z}}$ *with* $\tau = \frac{D^{(1)}a(1)}{2}$*, if and only if it generates* Π_g^1 *and*

$$D^{(j)}a(1) = 2\prod_{h=0}^{j-1}(\tau - h), \quad j = 1, ..., g.$$

The following result recently appeared as a natural generalization of the previous proposition.

Proposition 2.2. *[4, 6] A d-variate (*$d \geq 1$*) subdivision scheme* $\mathcal{S}_{\mathbf{a}}$

(i) generates Π_g^d *if and only if*

$$a(\mathbf{1}) = 2^d, \quad a(\mathbf{u}) = 0 \quad \textit{for} \;\; \mathbf{u} \in U := \{e^{-i\pi\xi}, \, \xi \in \Xi\}\backslash\{\mathbf{1}\}$$

and

$$D^{\mathbf{j}}a(\mathbf{u}) = 0 \quad \textit{for} \;\; \mathbf{u} \in U, \;\; \mathbf{j} = (j_1, ..., j_d) \in \mathbb{N}_0^d \;\; \textit{with} \;\; j_1 + ... + j_d \leq g;$$

(ii) reproduces Π_g^d *with respect to the parametrization* $\{\mathbf{t}_{\mathbf{i}}^{(k)} = \frac{\mathbf{i}+\boldsymbol{\tau}}{2^k}\}_{\mathbf{i}\in\mathbb{Z}^d}$ *with* $\boldsymbol{\tau}$ *in* (2.2)*, if and only if it generates* Π_g^d *and*

$$D^{\mathbf{j}}a(\mathbf{1}) = 2^d \prod_{\ell=1}^{d}\prod_{h_\ell=0}^{j_\ell-1}(\tau_\ell - h_\ell) \quad \textit{for} \;\; \mathbf{j} = (j_1, ..., j_d) \in \mathbb{N}_0^d \;\; \textit{with} \;\; j_1 + ... + j_d \leq g.$$

2.2. Refine-and-Smooth (RS) subdivision schemes

Refine-and-Smooth algorithms define a subdivision process where each subdivision step $\mathcal{S}_{\mathbf{a}} : \mathbf{P}^{(k-1)} \to \mathbf{P}^{(k)}$ first refines the current data and then applies n smoothing stages to the refined data, as shown in the following algorithm.

Algorithm 1.

A Refine-and-Smooth (*RS*) algorithm

Input: $\mathbf{P}^{(0)}$ initial data;
$k^* \in \mathbb{N}$ number of subdivision steps;
$n \in \mathbb{N}$ number of smoothing stages;

For $k = 1, \ldots, k^*$
- Set $\mathbf{P}^{k-1,0} := \mathbf{P}^{(k-1)}$
- Apply the *refine stage* (R): $\mathbf{P}^{k-1,1} = R\,\mathbf{P}^{k-1,0}$
- Apply n *smoothing stages* (S): $\mathbf{P}^{k-1,\ell+1} = S\,\mathbf{P}^{k-1,\ell}, \;\; \ell = 1, \ldots, n$
- Set $\mathbf{P}^{(k)} := \mathbf{P}^{k-1,n+1}$

Output: $\mathbf{P}^{(k^*)}$ k^*-th level subdivided data

Since the subdivision step $\mathcal{S}_{\mathbf{a}} : \mathbf{P}^{(k-1)} \to \mathbf{P}^{(k)}$ can be represented in terms of Laurent polynomials via

$$p^{(k)}(z) = a(z)\, p^{(k-1)}(z^2)$$

where

$$p^{(k-1)}(z) = \sum_{\mathbf{i}\in\mathbb{Z}^d} p_{\mathbf{i}}^{(k-1)} z^{\mathbf{i}}, \quad z \in (\mathbb{C}\backslash\{0\})^d,$$

it turns out that the symbol associated to a *RS* algorithm featured by n smoothing stages is given by

$$a_n(z) = (s(z))^n\, r(z), \quad n \in \mathbb{N}.$$

The most famous family of *RS* algorithms is the one proposed by Lane and Riesenfeld [19], generating in the limit degree-$(n+1)$ uniform B-splines. This proposal is featured by a refine and a smoothing stage both based on local linear interpolation. In fact, in the univariate case ($d = 1$), $r(z) = \frac{(1+z)^2}{2}$ is the symbol of the interpolating 2-point scheme (i.e., the linear B-spline scheme) and $s(z) = r_{odd}(z) = \frac{1+z}{2}$ coincides with its odd subsymbol, so that

$$a_n(z) = \frac{(1+z)^{n+2}}{2^{n+1}}, \quad n \in \mathbb{N}. \tag{2.3}$$

The authors of [1] called the family of Lane-Riesenfeld's schemes *L-schemes*, to stress the connection of the refine and smoothing stage definition with *linear* interpolation. In that paper they also generalized Lane-Riesenfeld's idea by using a higher-order local interpolation operator, both for the refine and the successive smoothing stages. In particular, they studied the case where the local cubic operator that stems from Dubuc-Deslauriers interpolating 4-point scheme [11] is used, and called the new family of schemes *C-schemes*. The n-th member of this family has symbol

$$a_n(z) = \frac{(1+z)^{n+4}}{2^{n+3}} \left(-\frac{z^2}{8} + \frac{5}{4}z - \frac{1}{8}\right)^n \left(-\frac{z^2}{2} + 2z - \frac{1}{2}\right), \quad n \in \mathbb{N} \tag{2.4}$$

being

$$r(z) = -\frac{1}{16}z^6 + \frac{9}{16}z^4 + z^3 + \frac{9}{16}z^2 - \frac{1}{16} = \frac{(1+z)^4}{2^3}\left(-\frac{z^2}{2} + 2z - \frac{1}{2}\right)$$

the symbol of the Dubuc-Deslauriers interpolating 4-point scheme and

$$s(z) = r_{odd}(z) = -\frac{1}{16}z^3 + \frac{9}{16}z^2 + \frac{9}{16}z - \frac{1}{16} = \frac{1+z}{2}\left(-\frac{z^2}{8} + \frac{5}{4}z - \frac{1}{8}\right)$$

the odd subsymbol of $r(z)$.

Remark 2. *When $n = 1$ the symbols of L-schemes and C-schemes can be written as $a_1(z) = r_{odd}(z)\, r(z)$, with $r(z)$ the symbol of a primal (interpolatory) scheme and $r_{odd}(z)$ the symbol associated to its odd rule. Applying the results in [9] there follows that the subdivision scheme having symbol $a_1(z)$ is nothing but the de Rham transform of the subdivision scheme with symbol $r(z)$, and thus it turns out to be a dual approximating scheme.*

In the next section we investigate another variant of Lane-Riesenfeld algorithm that, compared with the one proposed in [1], modifies only the refine stage. In fact, we consider the family of *RS* algorithms where, like in the well-known Lane-Riesenfeld algorithm, the smoothing stage S consists in performing averages of adjacent vertices, but, differently from the Lane-Riesenfeld algorithm, we apply a refine stage R based on a perturbation of Chaikin's corner cutting algorithm [3]. This modification produces a new family of alternating primal/dual univariate subdivision algorithms and their bivariate analogs for quadrilateral meshes of arbitrary topology, both characterized by the presence of a tension parameter w that allows for considerable variations of shape.

3. A new family of *RS* curve subdivision schemes with tension parameter

We denote by $\mathbf{P}^{k-1,0} = \{\mathbf{p}_i^{k-1,0}\}_{i\in\mathbb{Z}}$ the control points obtained from the $(k-1)$-th subdivision step and, using the well-known formulas

$$\begin{array}{rcl} \tilde{\mathbf{p}}_{2i}^{k-1,1} & = & \frac{1}{4}\mathbf{p}_{i-1}^{k-1,0} + \frac{3}{4}\mathbf{p}_i^{k-1,0}, \\ \tilde{\mathbf{p}}_{2i+1}^{k-1,1} & = & \frac{3}{4}\mathbf{p}_i^{k-1,0} + \frac{1}{4}\mathbf{p}_{i+1}^{k-1,0}, \end{array} \tag{3.1}$$

we compute the Chaikin's points $\tilde{\mathbf{p}}_{2i}^{k-1,1}$ and $\tilde{\mathbf{p}}_{2i+1}^{k-1,1}$ defined around the vertex $\mathbf{p}_i^{k-1,0}$. Then, we define the positions of the even and odd vertices of $\mathbf{P}^{k-1,1}$ (the polygon resulting from the application of the refine operator R to the data $\mathbf{P}^{(k-1)} \equiv \mathbf{P}^{k-1,0}$) by

$$\begin{array}{rcl} \mathbf{p}_{2i}^{k-1,1} & = & \mathbf{p}_i^{k-1,0} + 2w\,\mathbf{d}_{2i}^{k-1,1}, \\ \mathbf{p}_{2i+1}^{k-1,1} & = & \mathbf{p}_i^{k-1,0} + 2w\,\mathbf{d}_{2i+1}^{k-1,1}, \end{array} \qquad \text{with } w \in \mathbb{R}, \tag{3.2}$$

i.e., we correct the position of the vertex $\mathbf{p}_i^{k-1,0}$ by the vectors $2w\,\mathbf{d}_{2i}^{k-1,1}$ and $2w\,\mathbf{d}_{2i+1}^{k-1,1}$, respectively (see Figure 1), where

$$\mathbf{d}_{2i}^{k-1,1} = 2(n+3)\tilde{\mathbf{v}}_{2i}^{k-1,1} + (n-1)\mathbf{e}_{i-1,i}^{k-1,0}, \qquad \mathbf{d}_{2i+1}^{k-1,1} = 2(n+3)\tilde{\mathbf{v}}_{2i+1}^{k-1,1} + (n-1)\mathbf{e}_{i,i+1}^{k-1,0}, \qquad \text{with } n \in \mathbb{N}, \tag{3.3}$$

and

$$\begin{array}{rcl} \tilde{\mathbf{v}}_{2i}^{k-1,1} & = & \tilde{\mathbf{p}}_{2i}^{k-1,1} - \frac{\tilde{\mathbf{p}}_{2i}^{k-1,1}+\tilde{\mathbf{p}}_{2i+1}^{k-1,1}}{2}, \qquad \mathbf{e}_{i-1,i}^{k-1,0} = \mathbf{p}_i^{k-1,0} - \frac{\mathbf{p}_{i-1}^{k-1,0}+\mathbf{p}_i^{k-1,0}}{2}, \\ \tilde{\mathbf{v}}_{2i+1}^{k-1,1} & = & \tilde{\mathbf{p}}_{2i+1}^{k-1,1} - \frac{\tilde{\mathbf{p}}_{2i}^{k-1,1}+\tilde{\mathbf{p}}_{2i+1}^{k-1,1}}{2}, \qquad \mathbf{e}_{i,i+1}^{k-1,0} = \mathbf{p}_i^{k-1,0} - \frac{\mathbf{p}_i^{k-1,0}+\mathbf{p}_{i+1}^{k-1,0}}{2}. \end{array} \tag{3.4}$$

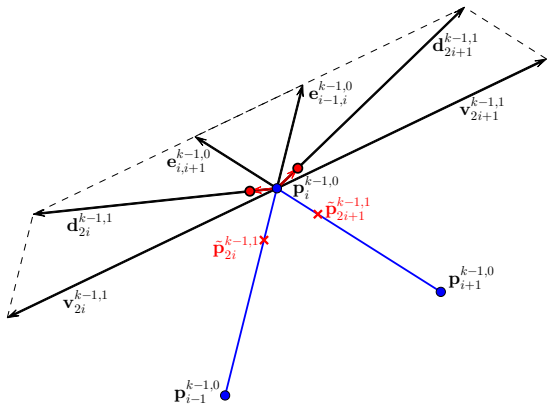

Figure 1: Geometric interpretation of the refine stage $R_{n,w}$ in (3.2) in the case $n = 2$ and $w = \frac{1}{18}$. The red bullets denote the vertices $\mathbf{p}_{2i}^{k-1,1}$ and $\mathbf{p}_{2i+1}^{k-1,1}$. For the sake of clarity the scaled vectors $\mathbf{v}_{2i+j}^{k-1,1} = 2(n+3)\tilde{\mathbf{v}}_{2i+j}^{k-1,1}$, $j = 0, 1$ are displayed in the picture. (For interpretation of the references to color in this figure legend, the reader is referred to the web version of this article.)

Combining all above formulas (3.1)-(3.4), the vertices $\mathbf{p}_{2i}^{k-1,1}$ and $\mathbf{p}_{2i+1}^{k-1,1}$ are practically computed by affine combinations of the vertices $\mathbf{p}_{i-1}^{k-1,0}$, $\mathbf{p}_i^{k-1,0}$, $\mathbf{p}_{i+1}^{k-1,0}$ of the form

$$\begin{array}{rcl} \mathbf{p}_{2i}^{k-1,1} & = & \frac{w}{2}(5-n)\,\mathbf{p}_{i-1}^{k-1,0} + \Big(1 + w(n-1)\Big)\,\mathbf{p}_i^{k-1,0} - \frac{w}{2}(n+3)\,\mathbf{p}_{i+1}^{k-1,0}, \\ \mathbf{p}_{2i+1}^{k-1,1} & = & -\frac{w}{2}(n+3)\,\mathbf{p}_{i-1}^{k-1,0} + \Big(1 + w(n-1)\Big)\,\mathbf{p}_i^{k-1,0} + \frac{w}{2}(5-n)\,\mathbf{p}_{i+1}^{k-1,0}. \end{array} \tag{3.5}$$

There follows that the refine stage mapping the polygon $\mathbf{P}^{k-1,0}$ into $\mathbf{P}^{k-1,1}$ is indeed dependent on the free parameter $w \in \mathbb{R}$ as well as on the number n of smoothing stages S that will be successively performed, as described in Algorithm

1, in order to obtain the k-level points $\mathbf{P}^{(k)}$. Thus, from now on we will denote it by $R_{n,w}$.
Figure 2 aims at showing that, independently of the choice of n, the parameter w acts as a tension parameter since the smaller is the value of w, the closer the points $\mathbf{p}_{2i}^{k-1,1}, \mathbf{p}_{2i+1}^{k-1,1}$ will stay to $\mathbf{p}_i^{k-1,0}$, as described by equation (3.2).

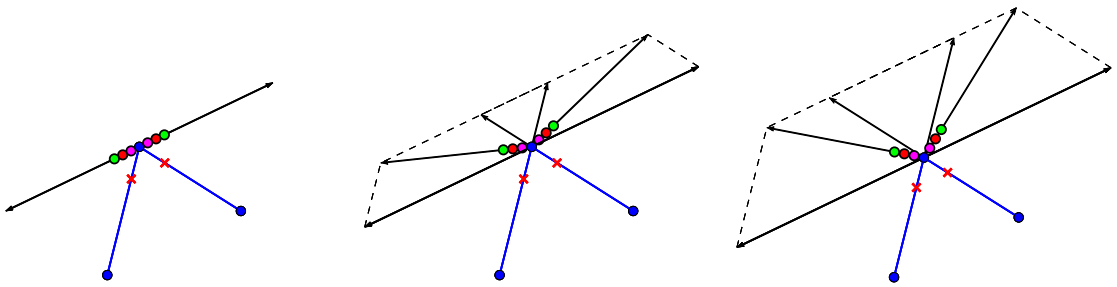

(a) (b) (c)

Figure 2: The role played by the parameters w and n in the refine stage $R_{n,w}$ when applied to the polygon $\mathbf{P}^{k-1,0}$ (blue polyline): (a) $n = 1$; (b) $n = 2$; (c) $n = 3$. Red crosses represent the Chaikin's points $\tilde{\mathbf{p}}_{2i}^{k-1,1}, \tilde{\mathbf{p}}_{2i+1}^{k-1,1}$. Magenta, red and green bullets show the pair of points $\mathbf{p}_{2i}^{k-1,1}, \mathbf{p}_{2i+1}^{k-1,1}$ in the case $w = \frac{1}{32}$, $w = \frac{1}{16}$ and $w = \frac{3}{32}$, respectively. (For interpretation of the references to color in this figure legend, the reader is referred to the web version of this article.)

Differently, the dependence of the refine operator on the number n of smoothing stages is introduced in order to modify the directions $\mathbf{d}_{2i}^{k-1,1}, \mathbf{d}_{2i+1}^{k-1,1}$ along which the vertices $\mathbf{p}_{2i}^{k-1,1}, \mathbf{p}_{2i+1}^{k-1,1}$ will be respectively inserted. To understand the role played by the parameter n in the refine stage, let us observe that, in view of (3.4) and (3.1), we can write

$$\tilde{\mathbf{v}}_{2i}^{k-1,1} = \frac{1}{2}\left(\tilde{\mathbf{p}}_{2i}^{k-1,1} - \tilde{\mathbf{p}}_{2i+1}^{k-1,1}\right) = \frac{1}{8}\left(\mathbf{p}_{i-1}^{k-1,0} - \mathbf{p}_{i+1}^{k-1,0}\right),$$

and then $\mathbf{v}_{2i}^{k-1,1} = 2(n+3)\tilde{\mathbf{v}}_{2i}^{k-1,1}$ is parallel to $\mathbf{p}_{i-1}^{k-1,0} - \mathbf{p}_{i+1}^{k-1,0}$. Thus, the height h_n of the parallelogram formed by $\mathbf{v}_{2i}^{k-1,1}$ and $(n-1)\mathbf{e}_{i-1,i}^{k-1,0}$ (see Figure 3) can be computed as

$$h_n = (n-1)\|\mathbf{e}_{i-1,i}^{k-1,0}\|_2 \ \sin\theta$$

with $\|\mathbf{e}_{i-1,i}^{k-1,0}\|_2 = \frac{1}{2}\,\|\mathbf{p}_i^{k-1,0} - \mathbf{p}_{i-1}^{k-1,0}\|_2$ and $\theta = \angle(\mathbf{p}_i^{k-1,0}, \mathbf{p}_{i-1}^{k-1,0}, \mathbf{p}_{i+1}^{k-1,0})$. There follows that the greater the value of $n \in \mathbb{N}$, the longer the segment h_n. This means that the greater the value of n, the more distant the point $\mathbf{p}_{2i}^{k-1,1}$ will be placed from the line passing through $\mathbf{p}_i^{k-1,0}$ that is parallel to $\mathbf{p}_{i-1}^{k-1,0} - \mathbf{p}_{i+1}^{k-1,0}$ (see Figures 2 and 3). Since the same reasoning applies also to the parallelogram formed by $\mathbf{v}_{2i+1}^{k-1,1}$ and $(n-1)\mathbf{e}_{i,i+1}^{k-1,0}$, the point $\mathbf{p}_{2i+1}^{k-1,1}$ will have analogous behaviour.

Remark 3. *Note that, when $n = 1$, $h_1 = 0$ and hence the points $\mathbf{p}_{2i}^{k-1,1}$ and $\mathbf{p}_{2i+1}^{k-1,1}$ are placed exactly on the line passing through $\mathbf{p}_i^{k-1,0}$ that is parallel to $\mathbf{p}_{i-1}^{k-1,0} - \mathbf{p}_{i+1}^{k-1,0}$ (see Figure 2).*

Exploiting the formalism of Laurent polynomials as discussed in Section 2.2, we have that, as a straightforward consequence of (3.5), the symbol associated to the refine stage $R_{n,w}$ reads as

$$r_{n,w}(z) = \frac{1+z}{2}\Big(- w(n+3)z^4 + 8wz^3 + 2(w(n-5)+1)z^2 + 8wz - w(n+3)\Big).$$

Assuming that the smoothing stage S simply performs averages of adjacent vertices as in the Lane-Riesenfeld algorithm, i.e. has symbol $s(z) = \frac{1+z}{2}$, then the new family of RS subdivision schemes, hereinafter denoted by $\{\mathcal{S}_{\mathbf{a}_{n,w}}\}_{n\in\mathbb{N}}$, can be conveniently described by the two-parameter symbol

$$a_{n,w}(z) = \Big(s(z)\Big)^n r_{n,w}(z) = \left(\frac{1+z}{2}\right)^{n+1}\Big(- w(n+3)z^4 + 8wz^3 + 2(w(n-5)+1)z^2 + 8wz - w(n+3)\Big). \tag{3.6}$$

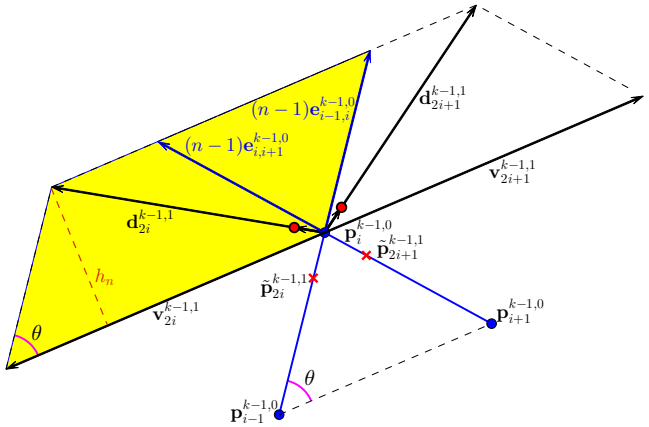

Figure 3: Geometric interpretation of the role played by the parameter n in the refine stage $R_{n,w}$ when applied to the polygon $\mathbf{P}^{k-1,0}$.

Here, $n \in \mathbb{N}$ is the parameter that accounts for smoothness by means of the number of applied smoothing stages, and is thus used to identify the family member, whereas $w \in \mathbb{R}$ is the tension parameter that can be used to modify the shape of the limit curves generated by each family member.

Remark 4. *When $w = 0$ the symbol $a_{n,w}(z)$ in (3.6) reduces to the Laurent polynomial of a degree-n B-spline.*

Moreover, it is worthwhile to notice that the first two members of the new family in (3.6) are two well-known subdivision schemes with tension parameter, proposed in the literature via isolated constructions. More precisely:

- when $n = 1$, (3.6) yields the symbol of the interpolatory 4-point scheme with tension parameter proposed in [14], having mask $\mathbf{a}_{1,w} = (-w, 0, w + \frac{1}{2}, 1, w + \frac{1}{2}, 0, -w)$;
- when $n = 2$, (3.6) yields the symbol of the dual approximating 4-point scheme with tension parameter proposed in [16], whose mask is $\mathbf{a}_{2,w} = \frac{1}{8}(-5w, -7w, 3w + 2, 9w + 6, 9w + 6, 3w + 2, -7w, -5w)$.

3.1. Properties of the new family of RS curve subdivision schemes with tension parameter

We start by studying the smoothness properties of the family of subdivision schemes $\{\mathcal{S}_{\mathbf{a}_{n,w}}\}_{n\in\mathbb{N}}$. The next proposition follows the reasoning in [1, Section 3.3] to derive a lower bound on the Hölder regularity. Its proof is thus omitted since it trivially consists in the application of a known general result to the symbol we deal with.

Proposition 3.1. *The subdivision scheme $\mathcal{S}_{\mathbf{a}_{n,w}}$ having symbol $a_{n,w}(z) = \left(\frac{1+z}{2}\right)^{n+1} b_{n,w}(z)$ with $b_{n,w}(z) = -w(n+3)z^4 + 8wz^3 + 2\Big((n-5)w + 1\Big)z^2 + 8wz - w(n+3)$, generates limit curves with Hölder regularity*

$$\mathcal{H} \geq n + 1 - \frac{\log_2(\|\mathbf{b}_{n,w}^{\ell}\|_\infty)}{\ell}, \quad \textit{for any } \ell \geq 1 \tag{3.7}$$

where $\mathbf{b}_{n,w}^{\ell}$ denotes the mask associated to the symbol $b_{n,w}^{\ell}(z) = b_{n,w}(z)\, b_{n,w}(z^2) \ldots b_{n,w}(z^{2^{\ell-1}})$, $\ell \geq 1$.

As a consequence of Proposition 3.1 we have that, for a fixed value of $n \in \mathbb{N}$, if w is chosen such that $\|\mathbf{b}_{n,w}^{\ell}\|_\infty < 2^\ell$ then $\log_2(\|\mathbf{b}_{n,w}^{\ell}\|_\infty) < \ell$ and $\mathcal{H} \geq n+1-\frac{\log_2(\|\mathbf{b}_{n,w}^{\ell}\|_\infty)}{\ell} > n$, that is $\mathcal{S}_{\mathbf{a}_{n,w}}$ generates C^n limit curves. Note also that, choosing w such that $\|\mathbf{b}_{n,w}^{\ell}\|_\infty < 2^\ell$ is equivalent to check the contractivity of the symbol $\frac{1}{2}b_{n,w}(z)$, as required by the sufficient condition for C^n smoothness given in [15, Corollary 4.14]. This reasoning provides the following result.

Proposition 3.2. *If we choose*

- $0 < w < \frac{1}{2}\left(\sqrt{\frac{n+4}{(n+3)^2}} - \frac{1}{n+3}\right)$ *when* $1 \le n \le 2$*;*
- $\frac{1}{32}\left(\frac{n-5}{n-1} - \sqrt{\frac{-39+54n+n^2}{(n-1)^2}}\right) < w < \frac{n-13}{16(n-1)}$ *when* $6 \le n \le 13$*;*
- $\frac{1}{32}\left(\frac{n-5}{n-1} - \sqrt{\frac{-39+54n+n^2}{(n-1)^2}}\right) < w < 0$ *when* $n \ge 14$*;*

then the subdivision scheme $\mathcal{S}_{\mathbf{a}_{n,w}}$ *is* C^n*.*

Proof: The claim follows by checking for which values of $w \in \mathbb{R}$ the condition $\|\mathbf{b}^2_{n,w}\|_\infty < 4$ is satisfied. ■

Remark 5. *As it is well-known, increasing the value of* ℓ *in* (3.7) *we can enlarge the range of* w *that yields* C^n *continuity of* $\mathcal{S}_{\mathbf{a}_{n,w}}$*. Additionally, we can also identify the parameter ranges for the subdivision schemes* $\mathcal{S}_{\mathbf{a}_{n,w}}$ *with* $n = 3, 4, 5$*, which do not appear in Proposition 3.2 since for them the condition* $\|\mathbf{b}^2_{n,w}\|_\infty < 4$ *is never satisfied.*

In the following proposition we show how, using the so-called Rioul's exact method presented in [17], for all $n \in \mathbb{N}$ and w in a certain range, we can compute the exact Hölder regularity of the scheme $\mathcal{S}_{\mathbf{a}_{n,w}}$.

Proposition 3.3. *If* $w \in \left(-\frac{n+3}{2(n+1)^2}, \frac{1}{16}\right)$*, then for all* $n \in \mathbb{N}$ *the Hölder regularity of the scheme* $\mathcal{S}_{\mathbf{a}_{n,w}}$ *is*

$$\mathcal{H} = n - log_2(\rho) \quad with \quad \rho = \frac{1}{2}\left(1 + w(n-1) + \sqrt{(n^2 - 34n + 33)w^2 + 2(n-9)w + 1}\right).$$

Proof: We rewrite the symbol $a_{n,w}(z)$ in (3.6) in the form

$$a_{n,w}(z) = \frac{(1+z)^{n+1}}{2^n} m_{n,w}(z) \quad \text{with} \quad m_{n,w}(z) = \sum_{j=0}^{4} m_j^{n,w} z^j = -\frac{w}{2}(n+3)z^4 + 4wz^3 + \Big((n-5)w+1\Big)z^2 + 4wz - \frac{w}{2}(n+3). \quad (3.8)$$

In view of the symbol factorization in (3.8), it follows that the Fourier transform of $\mathbf{m}_{n,w} = (m_0^{n,w},\, m_1^{n,w},\, m_2^{n,w},\, m_3^{n,w},\, m_4^{n,w})$ given by

$$M_{n,w}(\zeta) = m_{n,w}(e^{-\mathrm{i}\zeta}) = \sum_j m_j^{n,w}\, e^{-\mathrm{i}j\zeta} = 1 + 2w(n-1) + 8w\cos(\zeta) - 2w(n+3)\cos^2(\zeta), \qquad \zeta \in \mathbb{R}$$

is both periodic with period 2π and real. Since when $w \in \left(-\frac{n+3}{2(n+1)^2}, \frac{1}{16}\right)$ we have $M_{n,w}(\zeta) > 0$ for all $\zeta \in [-\pi, \pi]$, then in view of [17, Theorem 2] the lower bound on the Hölder regularity is optimal. This means that for such values of w the Hölder regularity of the scheme $\mathcal{S}_{\mathbf{a}_{n,w}}$ is exactly $\mathcal{H} = n - log_2(\rho)$ with ρ denoting the spectral radius of the matrix

$$\mathcal{M} = \begin{pmatrix} 1 + w(n-5) & -w(n+3) \\ 4w & 4w \end{pmatrix}.$$

Being the eigenvalues of $\mathcal{M}$ given by $\frac{1}{2}\left(1 + w(n-1) \pm \sqrt{(n^2 - 34n + 33)w^2 + 2(n-9)w + 1}\right)$, it easily follows that for all $n \in \mathbb{N}$ and $w \in \left(-\frac{n+3}{2(n+1)^2}, \frac{1}{16}\right)$ the spectral radius of $\mathcal{M}$ is $\rho = \frac{1}{2}\left(1 + w(n-1) + \sqrt{(n^2 - 34n + 33)w^2 + 2(n-9)w + 1}\right)$. This concludes the proof. ■

Corollary 3.4. *Collecting the results in Proposition 3.2 and Proposition 3.3 we obtain that, if the free parameter* $w \in \mathbb{R}$ *is chosen in the following way*

- $0 < w < \frac{1}{2}\left(\sqrt{\frac{n+4}{(n+3)^2}} - \frac{1}{n+3}\right)$ *when* $n = 1, 2$*;*

- $-\frac{n+3}{2(n+1)^2} < w < \frac{n-5}{8(n-1)} \cup 0 < w < \frac{1}{16}$ *when* $3 \le n \le 5$*;*
- $\frac{1}{32}\left(\frac{n-5}{n-1} - \sqrt{\frac{-39+54n+n^2}{(n-1)^2}}\right) < w < 0 \cup \frac{n-5}{8(n-1)} < w < \frac{1}{16}$ *when* $6 \le n \le 9$*;*
- $\frac{1}{32}\left(\frac{n-5}{n-1} - \sqrt{\frac{-39+54n+n^2}{(n-1)^2}}\right) < w < 0$ *when* $n \ge 10$*;*

then the subdivision scheme $\mathcal{S}_{\mathbf{a}_{n,w}}$ *is* C^n*.*

Proof: We start by observing that the following conditions on w

- $0 < w < \frac{1}{16}$ when $n = 1, 2$;
- $-\frac{n+3}{2(n+1)^2} < w < \frac{n-5}{8(n-1)} \cup 0 < w < \frac{1}{16}$ when $3 \le n \le 5$;
- $-\frac{n+3}{2(n+1)^2} < w < 0 \cup \frac{n-5}{8(n-1)} < w < \frac{1}{16}$ when $6 \le n \le 9$;
- $-\frac{n+3}{2(n+1)^2} < w < 0$ when $n \ge 10$;

satisfy at the same time the two inequalities $-\frac{n+3}{2(n+1)^2} < w < \frac{1}{16}$ and $\rho < 1$, i.e. $\log_2(\rho) < 0$, so that, in view of Proposition 3.3, the Hölder regularity of the scheme $\mathcal{S}_{\mathbf{a}_{n,w}}$ is $\mathcal{H} = n - \log_2(\rho) > n$. Thus the claim is obtained considering the union of the ranges provided above and in Proposition 3.2. ■

Remark 6. *When* $w = \frac{1}{16}$ *the symbol of the family of schemes* $\{\mathcal{S}_{\mathbf{a}_{n,w}}\}_{n\in\mathbb{N}}$ *in* (3.6) *becomes*

$$a_{n,\frac{1}{16}}(z) = \frac{(1+z)^{n+3}}{2^{n+2}}\left(-\frac{n+3}{8}z^2 + \frac{n+7}{4}z - \frac{n+3}{8}\right), \quad n \in \mathbb{N} \tag{3.9}$$

which means that our family contains the Hormann-Sabin's family in [18] as a special subfamily. In view of the results in [18], the Hölder regularity of the subfamily $\{\mathcal{S}_{\mathbf{a}_{n,\frac{1}{16}}}\}_{n\in\mathbb{N}}$ *is given by*

$$\mathcal{H} = n + 3 - \log_2\left(\frac{n+7}{2}\right). \tag{3.10}$$

Without surprise we can observe that the first two family members of the subfamily $\{\mathcal{S}_{\mathbf{a}_{n,\frac{1}{16}}}\}_{n\in\mathbb{N}}$ *coincide with the Dubuc-Deslauriers interpolatory 4-point scheme in [11] having symbol* $a_{1,\frac{1}{16}}(z) = \left(\frac{1+z}{2}\right)^4\left(-\frac{1}{2}z^2 + 2z - \frac{1}{2}\right)$*, and the approximating dual 4-point scheme in [16] whose symbol is* $a_{2,\frac{1}{16}}(z) = 2\left(\frac{1+z}{2}\right)^5\left(-\frac{5}{8}z^2 + \frac{9}{4}z - \frac{5}{8}\right)$*.*

We continue by studying the properties of polynomial generation and polynomial reproduction satisfied by the new family of subdivision schemes $\{\mathcal{S}_{\mathbf{a}_{n,w}}\}_{n\in\mathbb{N}}$, whose n-th member is described by the symbol in (3.6). After introducing the notation $\Omega_n = \{w \in \mathbb{R} \,|\, \mathcal{S}_{\mathbf{a}_{n,w}} \text{ is convergent}\}$ and observing that, in view of Remark 6, $w = \frac{1}{16} \in \Omega_n$ for all $n \in \mathbb{N}$, we can formulate the following propositions.

Proposition 3.5. *The subdivision scheme* $\mathcal{S}_{\mathbf{a}_{n,w}}$ *generates* Π^1_n *for all* $n \in \mathbb{N}$ *and* $w \in \Omega_n$*. Moreover, if* $w = \frac{1}{16}$*,* $\mathcal{S}_{\mathbf{a}_{n,w}}$ *generates* Π^1_{n+2} *for all* $n \in \mathbb{N}$*.*

Proof: Since conditions

$$a_{n,w}(1) = 2, \quad a_{n,w}(-1) = 0, \quad D^{(\ell)}a_{n,w}(-1) = 0, \quad \ell = 1, ..., n \tag{3.11}$$

are verified by $a_{n,w}(z)$ independently of the value of w, then, in view of Proposition 2.1-case (i) generation of degree-n polynomials is obtained for all $w \in \Omega_n$. Moreover, since when setting $w = \frac{1}{16}$ two more $(1+z)$ terms can be factored out from $r_{n,w}(z)$, it easily follows that also $D^{(n+1)}a_{n,w}(-1) = D^{(n+2)}a_{n,w}(-1) = 0$, which concludes the proof. ■

Proposition 3.6. *If applying the parameter shift* $\tau = \frac{n+5}{2}$*, the subdivision scheme* $\mathcal{S}_{\mathbf{a}_{n,w}}$ *reproduces* Π_1^1 *with respect to the parametrization in* (2.1)*, for all* $n \in \mathbb{N}$ *and* $w \in \Omega_n$*. Moreover, if* $w = \frac{1}{16}$*,* $\mathcal{S}_{\mathbf{a}_{n,w}}$ *reproduces* Π_3^1 *for all* $n \in \mathbb{N}$*.*

Proof: Since the condition $D^{(1)}a_{n,w}(1) = n + 5$ is verified by the symbol $a_{n,w}(z)$ independently of the value of w, together with all conditions in (3.11), then in view of Proposition 2.1-case (*ii*) reproduction of linear polynomials is obtained for all $w \in \Omega_n$ with the parameter shift $\tau = \frac{n+5}{2}$. We conclude by observing that when $w = \frac{1}{16}$ the following two more conditions

$$D^{(2)}a_{n,w}(z)|_{z=1} = 2\tau(\tau - 1), \quad D^{(3)}a_{n,w}(z)|_{z=1} = 2\tau(\tau - 1)(\tau - 2)$$

are satisfied for all $n \in \mathbb{N}$, and thus reproduction of Π_3^1 is obtained. ■

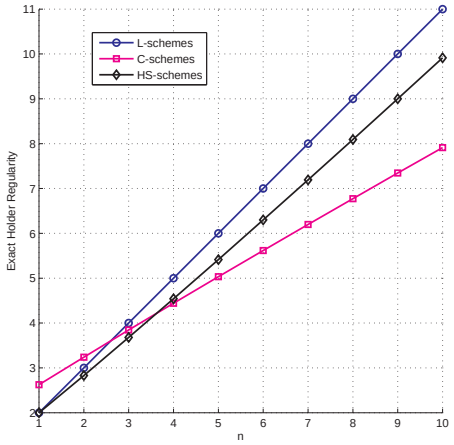

Figure 4: Comparison between the exact Hölder regularity of L-schemes in (2.3), C-schemes in (2.4) and HS-schemes in (3.9) for $n = 1, ..., 10$.

RS-schemes with $n \leq 8$ smoothing stages	BLF Support Width	Integer Smoothness (C^s)	Generation degree	Reproduction degree
L-schemes (deg-$(n+1)$ B-splines)	$n+2$	$s = n$	$n+1$	1
$\mathcal{S}_{\mathbf{a}_{n,w}}$	$n+5$	$s = n$	n	1
$\mathcal{S}_{\mathbf{a}_{n,\frac{1}{16}}}$ (HS-schemes)	$n+5$	$s = n$	$n+2$	3
C-schemes	$3n+6$	$s = \begin{cases} n+1 & \text{if } n \leq 2 \\ n & \text{if } n = 3,4,5 \\ < n & \text{otherwise} \end{cases}$	$n+3$	3

Table 1: Comparison between properties of L-schemes, C-schemes, HS-schemes and the new family of schemes $\mathcal{S}_{\mathbf{a}_{n,w}}$ with tension parameter.

It is obvious to emphasize that the Refine-and-Smooth algorithms which turn out to be more interesting in applications are the ones obtained with a not too high number of smoothing stages since the greater is n the larger becomes the support width of the basic limit function (BLF) and consequently the computational cost for generating curves. With this observation in mind it is worthwhile to notice that, when $n \leq 8$, by slightly increasing the support width of L-schemes, the new family of schemes allows us to introduce a tension parameter that can be used to control the shape of the limit curve without affecting the integer smoothness and the degree of polynomial reproduction. As we have already seen, when the free parameter w is set to $\frac{1}{16}$, the resulting subfamily of schemes $\{\mathcal{S}_{\mathbf{a}_{n,\frac{1}{16}}}\}_{n\in\mathbb{N}}$ (also denoted by HS-schemes) allows us to increase the degree of polynomial reproduction of the parameter-dependent family up to 3, without influencing the class of integer smoothness. In fact, in view of (3.10), for $n \leq 8$ HS-schemes have the same integer smoothness as L-schemes and at least the same integer smoothness as C-schemes whenever $n > 2$ (see Figure

4). Moreover, if applying the same number of smoothing stages, HS-schemes allow, on the one hand, to increase the degree of polynomial generation and reproduction of L-schemes in exchange of a slight increase of the support width and, on the other hand, to achieve the same degree of polynomial reproduction of C-schemes by means of a basic limit function with a remarkably smaller support width (see Table 1). Thus, in summary, we can conclude that HS-schemes are a good compromise between L-schemes and C-schemes and may be conveniently taken as building blocks for the derivation of bivariate subdivision schemes generating surfaces of arbitrary topology.

4. A new family of bivariate *RS* subdivision schemes for quadrilateral meshes

The generalization of Chaikin's scheme to polyhedral meshes is given by the so-called Doo-Sabin's subdivision scheme [2]. If the face to be subdivided is quadrilateral and its vertices are labeled as $\mathbf{p}_j^{k-1,0}$, $j = 0, ..., 3$, then the subdivision rules are simply given by the tensor product of Chaikin's rules and read as

$$\tilde{\mathbf{p}}_i^{k-1,1} = \sum_{j=0}^{3} \nu_{i,j}\, \mathbf{p}_j^{k-1,0}, \quad i = 0, ..., 3 \qquad \text{with} \quad \nu_{i,j} = \begin{cases} \frac{9}{16}, & \text{if } j = i \ ; \\ \frac{3}{16}, & \text{if } |j-i| = 1 \ ; \\ \frac{1}{16}, & \text{otherwise} \end{cases} \tag{4.1}$$

see Figure 5(b). More generally, if the face is delimited by N vertices $\mathbf{p}_j^{k-1,0}$, $j = 0, ..., N-1$, then the subdivision rules are a natural extension of the ones in (4.1), given by the following affine combination

$$\tilde{\mathbf{p}}_i^{k-1,1} = \sum_{j=0}^{N-1} \nu_{i,j}\, \mathbf{p}_j^{k-1,0}, \quad i = 0, ..., N-1 \qquad \text{with} \quad \nu_{i,j} = \begin{cases} \frac{N+5}{4N}, & \text{if } j = i \ ; \\ \frac{3+2\cos(2\pi(i-j)/N)}{4N}, & \text{otherwise} \end{cases} \tag{4.2}$$

(see Figure 5 (a)-(c) for different values of N).

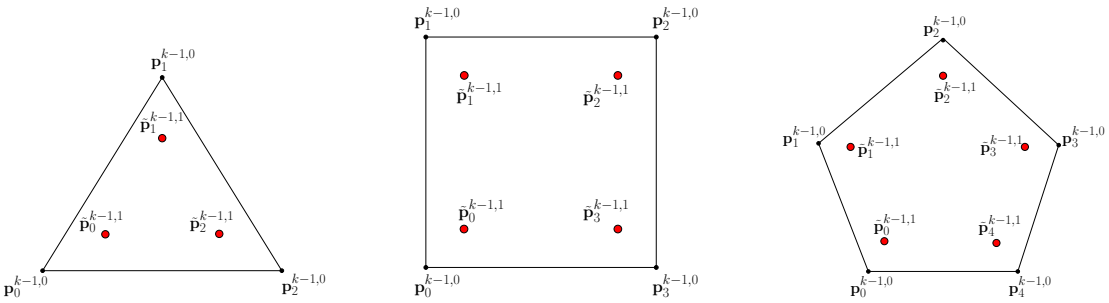

(a) $N = 3$ (b) $N = 4$ (c) $N = 5$

Figure 5: One step of Doo-Sabin's subdivision scheme for arbitrary faces with N vertices.

We continue by observing that, in the univariate case, we can conveniently combine the even and odd rules (3.2) describing the refine stage $R_{n,w} : \mathbf{P}^{k-1,0} \mapsto \mathbf{P}^{k-1,1}$, in the following single equation

$$\mathbf{p}_\ell^{k-1,1} = \mathbf{p}_*^{k-1,0} + 2w\, \mathbf{d}_\ell^{k-1,1} \qquad \ell = 1, 2 \tag{4.3}$$

with

$$\mathbf{d}_\ell^{k-1,1} = 2(n+3)\, \tilde{\mathbf{v}}_\ell^{k-1,1} + (n-1)\, \mathbf{e}_{\ell,*}^{k-1,0} \tag{4.4}$$

and

$$\tilde{\mathbf{v}}_\ell^{k-1,1} = \tilde{\mathbf{p}}_\ell^{k-1,1} - \mathcal{G}_*^{k-1,1}, \qquad \mathbf{e}_{\ell,*}^{k-1,0} = \mathbf{p}_*^{k-1,0} - \tilde{\mathcal{G}}_\ell^{k-1,0}, \tag{4.5}$$

where $\tilde{\mathbf{p}}_\ell^{k-1,1}$, $\ell = 1, 2$ denote the Chaikin's points in the neighborhood of $\mathbf{p}_*^{k-1,0}$, $\mathcal{G}_*^{k-1,1} = \frac{\tilde{\mathbf{p}}_1^{k-1,1} + \tilde{\mathbf{p}}_2^{k-1,1}}{2}$ denotes their midpoint and $\tilde{\mathcal{G}}_\ell^{k-1,0} = \frac{\mathbf{p}_\ell^{k-1,0} + \mathbf{p}_*^{k-1,0}}{2}$ the midpoint of the $(k-1)$-level points defining $\tilde{\mathbf{p}}_\ell^{k-1,1}$, as illustrated in Figure 6

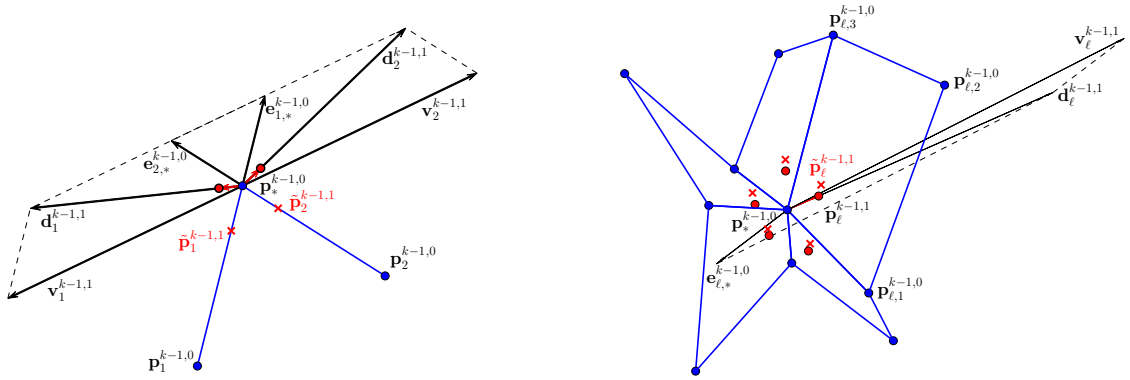

Figure 6: Geometric interpretation of the refine stage $R_{n,w}$ in the case $n = 2$: univariate case (left); bivariate case (right). The red crosses denote the Chaikin's/Doo-Sabin's points $\tilde{\mathbf{p}}_\ell^{k-1,1}$ whereas the red bullets the new vertices $\mathbf{p}_\ell^{k-1,1}$. For the sake of clarity the scaled vectors $\mathbf{v}_\ell^{k-1,1} = 2(n+3)\tilde{\mathbf{v}}_\ell^{k-1,1}$ are displayed in the picture. (For interpretation of the references to color in this figure legend, the reader is referred to the web version of this article.)

(left). This reformulation provides a straightforward extension of the refine stage to the bivariate case. In fact, in the case of quadrilateral meshes, if we consider a vertex $\mathbf{p}_*^{k-1,0}$ of arbitrary valence $N \geq 3$, the refine stage consists in deriving the new vertices $\tilde{\mathbf{p}}_\ell^{k-1,1}$, $\ell = 1, ..., N$ that the Doo-Sabin's scheme defines around it via the rules in (4.1), and in using them to compute the new points $\mathbf{p}_\ell^{k-1,1}$, $\ell = 1, ..., N$ via the following formula

$$\mathbf{p}_\ell^{k-1,1} = \mathbf{p}_*^{k-1,0} + 2w\,\mathbf{d}_\ell^{k-1,1} \qquad \ell = 1, ..., N \tag{4.6}$$

with $\mathbf{d}_\ell^{k-1,1}$ and $\tilde{\mathbf{v}}_\ell^{k-1,1}$, $\mathbf{e}_{\ell,*}^{k-1,0}$ as in equations (4.4) and (4.5), respectively. In this case $\mathcal{G}_*^{k-1,1} = \frac{\sum_{\ell=1}^N \tilde{\mathbf{p}}_\ell^{k-1,1}}{N}$ denotes the centroid of the Doo-Sabin's points in the neighborhood of $\mathbf{p}_*^{k-1,0}$, whereas $\tilde{\mathcal{G}}_\ell^{k-1,0} = \frac{\mathbf{p}_{\ell,1}^{k-1,0}+\mathbf{p}_{\ell,2}^{k-1,0}+\mathbf{p}_{\ell,3}^{k-1,0}+\mathbf{p}_*^{k-1,0}}{4}$ the centroid of the $(k-1)$-level points defining $\tilde{\mathbf{p}}_\ell^{k-1,1}$, as illustrated in Figure 6 (right).
The described computations provide an explicit definition of the vertex $\mathbf{p}_\ell^{k-1,1}$ via the following affine combination of the first ring of vertices placed around the extraordinary vertex $\mathbf{p}_*^{k-1,0}$

$$\begin{aligned}\mathbf{p}_\ell^{k-1,1} &= \Big(1 + \frac{3}{2}w(n-1)\Big)\mathbf{p}_*^{k-1,0} + \frac{w}{4N}\Big(((n+11)N - 3(n+3))\,(\mathbf{p}_{\ell,1}^{k-1,0} + \mathbf{p}_{\ell,3}^{k-1,0}) + ((5-n)N - (n+3))\,\mathbf{p}_{\ell,2}^{k-1,0}\Big) \\ &- \frac{w(n+3)}{4N}\sum_{j=1;j\neq\ell}^{N} 3(\mathbf{p}_{j,1}^{k-1,0} + \mathbf{p}_{j,3}^{k-1,0}) + \mathbf{p}_{j,2}^{k-1,0}, \qquad \ell = 1, \ldots, N. \end{aligned} \tag{4.7}$$

Like in the univariate case, in order to design a new family of tension-controlled *RS* subdivision algorithms for polyhedral meshes of arbitrary topology, we need to perform one refine stage $R_{n,w} : \mathbf{P}^{k-1,0} \mapsto \mathbf{P}^{k-1,1}$ as described in (4.7), followed by n smoothing stages $S : \mathbf{P}^{k-1,r} \mapsto \mathbf{P}^{k-1,r+1}$, $r = 1, ..., n$, each one consisting in computing local averages of the vertices of $\mathbf{P}^{k-1,r}$, as illustrated in Figure 7 for the cases $r = 1$ and $r = 2$. More precisely, Figure 7 shows that, for any given mesh of vertices $\mathbf{P}^{k-1,0}$, we first apply the refine operator R yielding a new mesh with vertices $\mathbf{P}^{k-1,1}$. Then, the application of one smoothing stage S to the resulting mesh consists in connecting the centers of all its adjacent faces, and all successive $n-1$ applications of the smoothing operator proceed analogously.

It is easy to see that, like in the univariate case, the family $\{\mathcal{S}_{\mathbf{a}_{n,w}}\}_{n\in\mathbb{N}}$ obtained from this construction includes an alternation of primal and dual schemes depending on the odd/even-ness of n. In the following two sections we focus our attention on the first two family members: $\mathcal{S}_{\mathbf{a}_{1,w}}$ and $\mathcal{S}_{\mathbf{a}_{2,w}}$.

5. A new non-tensor product interpolatory subdivision scheme with tension parameter

Applying the Refine-and-Smooth strategy illustrated in Section 4 with one smoothing stage only, we obtain an interpolatory subdivision scheme for quadrilateral meshes that, following the univariate notation, we denote by $\mathcal{S}_{\mathbf{a}_{1,w}}$.

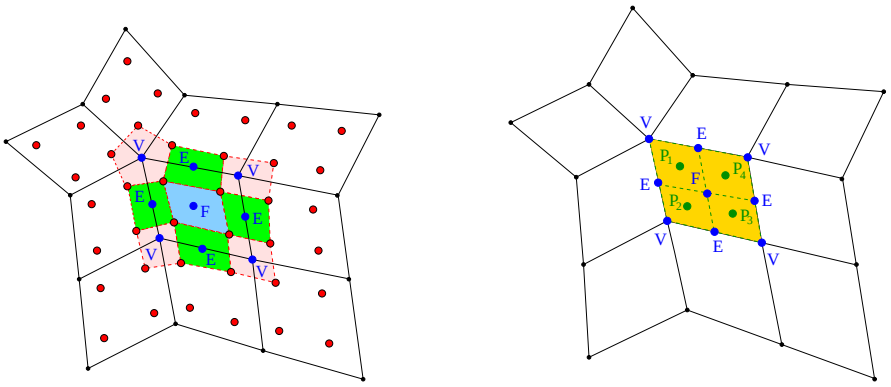

Figure 7: Illustration of the result of one smoothing stage (left) and two smoothing stages (right) in the neighborhood of an extraordinary vertex. Red bullets: vertices of $\mathbf{P}^{k-1,1}$ obtained from the refine stage $R_{n,w}$; blue bullets: vertices of $\mathbf{P}^{k-1,2}$, computed as the centroids of the marked faces having vertices in $\mathbf{P}^{k-1,1}$; green bullets: vertices of $\mathbf{P}^{k-1,3}$, computed as the centroids of the marked faces having vertices in $\mathbf{P}^{k-1,2}$. (For interpretation of the references to color in this figure legend, the reader is referred to the web version of this article.)

When setting $w = \frac{1}{16}$, the resulting interpolatory subdivision scheme coincides with the recent proposal in [10], but since any investigations on the distinctive features of the scheme have been conducted yet, in the remaining part of this section we study the main properties satisfied by the bivariate interpolatory subdivision scheme $\mathcal{S}_{\mathbf{a}_{1,w}}$, both in the regular case ($N = 4$) and in the neighborhood of extraordinary vertices of valence $N \neq 4$.

5.1. Properties of the regular case ($N = 4$)

When $N = 4$, the bivariate subdivision scheme $\mathcal{S}_{\mathbf{a}_{1,w}}$ has mask

$$\mathbf{a}_{1,w} = \begin{pmatrix} -\frac{w}{16} & -\frac{w}{8} & -\frac{7w}{16} & -\frac{3w}{4} & -\frac{7w}{16} & -\frac{w}{8} & -\frac{w}{16} \\ -\frac{w}{8} & 0 & \frac{w}{8} & 0 & \frac{w}{8} & 0 & -\frac{w}{8} \\ -\frac{7w}{16} & \frac{w}{8} & \frac{15w}{16}+\frac{1}{4} & \frac{3w}{4}+\frac{1}{2} & \frac{15w}{16}+\frac{1}{4} & \frac{w}{8} & -\frac{7w}{16} \\ -\frac{3w}{4} & 0 & \frac{3w}{4}+\frac{1}{2} & 1 & \frac{3w}{4}+\frac{1}{2} & 0 & -\frac{3w}{4} \\ -\frac{7w}{16} & \frac{w}{8} & \frac{15w}{16}+\frac{1}{4} & \frac{3w}{4}+\frac{1}{2} & \frac{15w}{16}+\frac{1}{4} & \frac{w}{8} & -\frac{7w}{16} \\ -\frac{w}{8} & 0 & \frac{w}{8} & 0 & \frac{w}{8} & 0 & -\frac{w}{8} \\ -\frac{w}{16} & -\frac{w}{8} & -\frac{7w}{16} & -\frac{3w}{4} & -\frac{7w}{16} & -\frac{w}{8} & -\frac{w}{16} \end{pmatrix}, \tag{5.1}$$

and symbol

$$\begin{aligned} a_{1,w}(z_1,z_2) &= \tfrac{1}{16}\, z_1^{-3}\, z_2^{-3}\, (1+z_1)^2\, (1+z_2)^2 \Big(-wz_1^4z_2^4 - 6wz_1^4z_2^2 - wz_1^4 + 4wz_1^3z_2^3 + 8wz_1^3z_2^2 + 4wz_1^3z_2 - 6wz_1^2z_2^4 \\ &+ 8wz_1^2z_2^3 - 4(5w-1)z_1^2z_2^2 + 8wz_1^2z_2 - 6wz_1^2 + 4wz_1z_2^3 + 8wz_1z_2^2 + 4wz_1z_2 - wz_2^4 - 6wz_2^2 - w\Big). \end{aligned} \tag{5.2}$$

Since $a_{1,w}(z_1,z_2) = a_{1,w}(z_2,z_1)$, then $\mathcal{S}_{\mathbf{a}_{1,w}}$ is a scheme with symmetry relative to the two axes, namely it is characterized by topologically equivalent rules for the computation of vertices corresponding to edges. However, it is a *non-tensor product* scheme since $a_{1,w}(z_1,z_2)$ cannot be written as the product of a polynomial in z_1 with a polynomial in z_2. Nevertheless, taking into account that $a_{1,w}(z_1,1)$ coincides with the interpolatory 4-point scheme in [14], the bivariate scheme with symbol $a_{1,w}(z_1,z_2)$ can be interpreted as a non-tensor product extension of the interpolatory 4-point scheme with tension parameter.

Remark 7. *Note that $a_{1,0}(z_1,z_2) = \frac{1}{4}\, z_1^{-1}\, z_2^{-1}\, (1+z_1)^2\, (1+z_2)^2$, namely when $w = 0$ the interpolatory subdivision scheme $\mathcal{S}_{\mathbf{a}_{1,w}}$ reduces to the tensor product of the linear B-spline scheme which is still interpolatory, but only C^0 (see Figure 8(a)).*

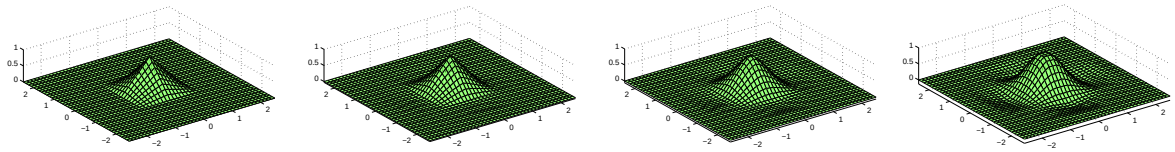

(a) $w = 0$ (b) $w = \frac{1}{32}$ (c) $w = \frac{1}{16}$ (d) $w = \frac{1}{8}$

Figure 8: Basic limit function of $\mathcal{S}_{\mathbf{a}_{1,w}}$ for different values of w.

The following proposition determines the parameter set $\Omega_1 = \{w \in \mathbb{R} \,|\, \mathcal{S}_{\mathbf{a}_{1,w}} \text{ is convergent}\}$ and shows that for w in a certain subset of Ω_1, the scheme $\mathcal{S}_{\mathbf{a}_{1,w}}$ produces C^1 limit surfaces when starting from any regular quadrilateral mesh. As usually done in the regular case $N = 4$, we analyze the smoothness of the limit surface via the formalism of Laurent polynomials. Since the symbol of the scheme $\mathcal{S}_{\mathbf{a}_{1,w}}$ contains the factors $(1 + z_1)^2$ and $(1 + z_2)^2$, with the aid of [15, Theorem 4.30] the following result can be easily proved.

Proposition 5.1. *If $w \in (-\frac{2}{9}, \frac{2}{15})$ the subdivision scheme $\mathcal{S}_{\mathbf{a}_{1,w}}$ converges to a continuous surface when starting from any regular quadrilateral mesh. Moreover, if $w \in (0, \frac{2}{15})$, the produced limit surface is C^1 continuous.*

Proof: Let us start by writing $a_{1,w}(z_1, z_2) = \left(\frac{1+z_1}{2}\right)^2 \left(\frac{1+z_2}{2}\right)^2 b_{1,w}(z_1, z_2)$ with

$$\begin{aligned} b_{1,w}(z_1, z_2) &= -wz_1^4z_2^4 - 6wz_1^4z_2^2 - wz_1^4 + 4wz_1^3z_2^3 + 8wz_1^3z_2^2 + 4wz_1^3z_2 - 6wz_1^2z_2^4 + 8wz_1^2z_2^3 \\ &- 4(5w-1)z_1^2z_2^2 + 8wz_1^2z_2 - 6wz_1^2 + 4wz_1z_2^3 + 8wz_1z_2^2 + 4wz_1z_2 - wz_2^4 - 6wz_2^2 - w. \end{aligned}$$

Since $a_{1,w}(z_1, z_2) = a_{1,w}(z_2, z_1)$, in view of [15, Theorem 4.30] we can determine the range of the parameter w which guarantees the convergence of the scheme $\mathcal{S}_{\mathbf{a}_{1,w}}$ by checking the contractivity of the scheme with symbol $\frac{1}{2}\left(\frac{1+z_1}{2}\right)^2 \left(\frac{1+z_2}{2}\right) b_{1,w}(z_1, z_2)$. This yields $w \in (-\frac{2}{9}, \frac{2}{15})$.
In the same spirit, the result on the C^1 continuity follows by checking the contractivity of the schemes with symbols $\frac{1}{2}\left(\frac{1+z_1}{2}\right)^2 b_{1,w}(z_1, z_2)$ and $\frac{1}{2}\left(\frac{1+z_1}{2}\right)\left(\frac{1+z_2}{2}\right) b_{1,w}(z_1, z_2)$. ■

In Figure 9 we illustrate the effect of the tension parameter w for values in the above determined range $(0, \frac{2}{15})$: the smaller is the value of w, the closer the limit surface stays to the initial mesh. This is clearly due to the fact that when $w \to 0$ the limit surface tends to the bi-linear B-spline surface (see Remark 7 as well as Figure 8).

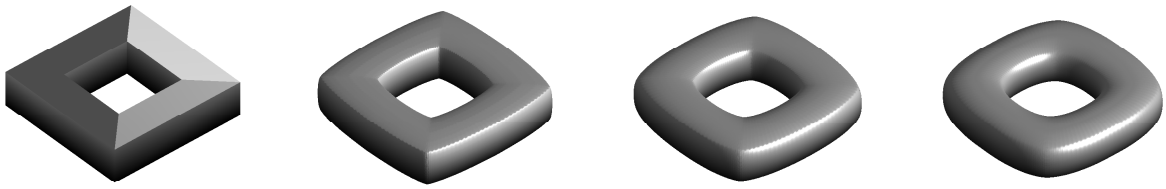

(a) initial mesh (b) $w = \frac{1}{32}$ (c) $w = \frac{1}{20}$ (d) $w = \frac{1}{16}$

Figure 9: Surfaces obtained by applying 6 iterations of the interpolatory subdivision scheme $\mathcal{S}_{\mathbf{a}_{1,w}}$ to the regular mesh in (a) for different values of $w \in (0, \frac{2}{15})$.

As a consequence of Proposition 5.1 we have that $\Omega_1 = \{w \in \mathbb{R} \,|\, \mathcal{S}_{\mathbf{a}_{1,w}} \text{ is convergent}\} = \left(-\frac{2}{9}, \frac{2}{15}\right)$. In the following two propositions we investigate the capability of the subdivision scheme $\mathcal{S}_{\mathbf{a}_{1,w}}$, with $w \in \Omega_1$, of generating and reproducing polynomials.

Proposition 5.2. *The subdivision scheme $\mathcal{S}_{\mathbf{a}_{1,w}}$ generates Π_1^2 for all $w \in \Omega_1$ and generates Π_3^2 for $w = \frac{1}{16}$.*

The detailed proof of Proposition 5.2 is given in Appendix A.

Remark 8. *It is interesting to observe that, since the subdivision scheme $\mathcal{S}_{\mathbf{a}_{1,\frac{1}{16}}}$ generates Π_3^2, then, in view of the results in [5], the symbol $z_1^3 z_2^3\, a_{1,\frac{1}{16}}(z_1, z_2)$ can be decomposed as*

$$z_1^3 z_2^3\, a_{1,\frac{1}{16}}(z_1, z_2) = 4 \sum_{B_{i,j,k} \in I_4} L_{i,j,k}\, \sigma_{i,j,k}(z_1, z_2)\, B_{i,j,k}(z_1, z_2),$$

where

- $B_{i,j,k}(z_1, z_2) = \left(\frac{1+z_1}{2}\right)^i \left(\frac{1+z_2}{2}\right)^j \left(\frac{1+z_1 z_2}{2}\right)^k$, $i, j, k \in \mathbb{N}_0$ *are normalized mask symbols of three-directional box-splines;*
- $I_4 = \{B_{4,4,0},\, B_{4,0,4},\, B_{0,4,4},\, B_{3,3,1},\, B_{3,1,3},\, B_{1,3,3},\, B_{2,2,2}\}$ *is the set of generators of* $\mathcal{I}^4 = \{p \in \Pi^2 \,:\, (D^{(j_1,j_2)}p)(\mathbf{u}) = 0$ *for* $\mathbf{u} \in \{(1,-1),\, (-1,1),\, (-1,-1)\},\ j_1 + j_2 < 4\}$*;*
- $\sigma_{i,j,k}(z_1, z_2)$ *are Laurent polynomials normalized by* $\sigma_{i,j,k}(1,1) = 1$*;*
- $L_{i,j,k}$ *are real coefficients that fulfill the condition* $\sum L_{i,j,k} = 1$.

More precisely, a representation of the symbol $z_1^3 z_2^3\, a_{1,\frac{1}{16}}(z_1, z_2)$ in terms of three-directional box-splines from the list I_4 is given by

$$z_1^3 z_2^3\, a_{1,\frac{1}{16}}(z_1, z_2) = 4\Big(L_{4,4,0}\, \sigma_{4,4,0}(z_1, z_2)\, B_{4,4,0}(z_1, z_2) + L_{3,3,1}\, \sigma_{3,3,1}(z_1, z_2)\, B_{3,3,1}(z_1, z_2) + L_{2,2,2}\, \sigma_{2,2,2}(z_1, z_2)\, B_{2,2,2}(z_1, z_2)\Big),$$

with

$$L_{4,4,0} = \frac{\theta_1(\theta_2+16)}{(\theta_1+\theta_2)(\theta_2-8)}, \qquad L_{3,3,1} = \frac{\theta_2(\theta_2+16)}{(\theta_1+\theta_2)(\theta_2-8)}, \qquad L_{2,2,2} = -\frac{24}{\theta_2-8},$$

and the normalized symbols

$$\begin{aligned}
\sigma_{4,4,0}(z_1, z_2) &= \tfrac{1}{4\theta_1(\theta_2+16)}\Big((\theta_1+\theta_2)(\theta_3-6(\theta_2-16))z_1^2 z_2^2 - (\theta_1+\theta_2)(\theta_2-8)(z_1^2+z_2^2)\\
&+ 2(6\theta_1\theta_2 - 24\theta_1 - 40\theta_2 + 5\theta_2^2)z_1 z_2 - 32\theta_2 - 2\theta_2^2 - \theta_1\theta_3 - \theta_2\theta_3\Big),\\
\sigma_{3,3,1}(z_1, z_2) &= \tfrac{1}{4\theta_2(\theta_2+16)}\Big(-(\theta_1+\theta_2)(\theta_3-6(\theta_2-16))z_1^2 z_2^2\\
&+ (\theta_1+\theta_2)(\theta_2-8)(z_1^2+z_2^2) + (16\theta_1 + 32\theta_2 - 5\theta_1\theta_2 - \theta_1\theta_3 - \theta_2\theta_3 - 4\theta_2^2)z_1 z_2\\
&+ (48\theta_1 + 64\theta_2 - 3\theta_1\theta_2 + \theta_1\theta_3 + \theta_2\theta_3 - 2\theta_2^2)(z_1+z_2) + \theta_2(3\theta_1 + 4\theta_2 + 16)\Big),\\
\sigma_{2,2,2}(z_1, z_2) &= \tfrac{1}{384}\Big((7\theta_2 - \theta_3 - 104)z_1^2 z_2^2 + (\theta_2+\theta_3+40)(z_1^2+z_2^2) - 16(\theta_2-14)z_1 z_2 + 96(z_1+z_2) + (7\theta_2 - \theta_3 - 8)\Big),
\end{aligned}$$

expressed in terms of the arbitrary coefficients $\theta_1, \theta_2, \theta_3 \in \mathbb{R}$. Since the generators $B_{4,4,0}(z_1, z_2)$, $B_{3,3,1}(z_1, z_2)$ and $B_{2,2,2}(z_1, z_2)$ are all multiples of $B_{2,2,0}(z_1, z_2)$, there follows that the symbol $z_1^3 z_2^3\, a_{1,\frac{1}{16}}(z_1, z_2)$ contains the factor $(1 + z_1)^2(1 + z_2)^2$, as can be noticed from equation (5.2).

Proposition 5.3. *If applying the parameter shift $(\tau_1, \tau_2) = (0, 0)$, the subdivision scheme $\mathcal{S}_{\mathbf{a}_{1,w}}$ reproduces Π_1^2 for all $w \in \Omega_1$ and reproduces Π_3^2 for $w = \frac{1}{16}$, with respect to the primal parametrization in* (2.1).

The reader may find the full proof of Proposition 5.3 in Appendix A.

5.2. Properties of the irregular case

In case the initial mesh contains some extraordinary vertices (i.e., vertices of valence $N \neq 4$), after a sufficiently high number of subdivision steps they become isolated in an otherwise regular tiling of the surface. Therefore, following the approach in [22], convergence and smoothness of the subdivision scheme can be obtained by analyzing the properties of the local subdivision matrix $\mathcal{A}$ defined in the neighborhood of the extraordinary vertex. Since in the regular case the parameter setting $w = \frac{1}{16}$ provides the scheme with the best behaviour, we conclude by analyzing the smoothness properties of the subdivision scheme $\mathcal{S}_{\mathbf{a}_{1,\frac{1}{16}}}$ when applied to an arbitrary quadrilateral mesh with extraordinary vertices of valence $N < 10$, as this is the case that actually occurs in most of the applications.

Proposition 5.4. *The subdivision scheme $\mathcal{S}_{\mathbf{a}_{1,\frac{1}{16}}}$ produces C^1 limit surfaces when applied to arbitrary quadrilateral meshes with extraordinary vertices of valence $N < 10$.*

Proof: Recalling the result in Proposition 5.1, we already know that the subdivision scheme $\mathcal{S}_{\mathbf{a}_{1,\frac{1}{16}}}$ produces C^1 limit surfaces in regular regions. Then, in order to study the behaviour of the scheme in the neighborhood of extraordinary vertices of valence $3 \leq N \leq 9$, we use the approach described in [22] which consists in analyzing the eigenstructure of the local subdivision matrix $\mathcal{A}$ defined in the neighborhood of the extraordinary vertex. As it is well-known, the local subdivision matrix $\mathcal{A}$ is a block circulant matrix of the form $\mathcal{A} = circ(\mathcal{A}_0^{(N)}, \mathcal{A}_1^{(N)}, ..., \mathcal{A}_{N-2}^{(N)}, \mathcal{A}_{N-1}^{(N)})$, and its eigenvalues coincide with the eigenvalues of the N Fourier blocks $\hat{\mathcal{A}}_\ell^{(N)} := \sum_{j=0}^{N-1} \left(e^{\frac{2\pi i}{N}}\right)^{j\ell} \mathcal{A}_j^{(N)}$, $\ell = 0, ..., N-1$. For the subdivision scheme $\mathcal{S}_{\mathbf{a}_{1,\frac{1}{16}}}$ the first leading eigenvalues of $\mathcal{A}$ satisfy $1 = \lambda_0 > \lambda_1 = \lambda_2$ with λ_0 being the dominant eigenvalue of $\hat{\mathcal{A}}_0^{(N)}$, λ_1 the dominant eigenvalue of $\hat{\mathcal{A}}_1^{(N)}$ and λ_2 that of $\hat{\mathcal{A}}_{N-1}^{(N)}$, and all remaining eigenvalues of $\mathcal{A}$ are strictly smaller than λ_2 in modulus (see Table 2). To conclude the proof we consider the limit surfaces generated by the so-called characteristic meshes (i.e., the control meshes provided by the two eigenvectors corresponding to the subdominant eigenvalues λ_1, λ_2), also known as the characteristic maps of the subdivision scheme. Since it has been numerically verified for all valencies $N < 10$ that such characteristic maps are all regular, i.e. have non-zero Jacobian determinant everywhere, and locally injective in the neighborhood of the extraordinary point (as also confirmed by Figure 10), there follows that C^1 regularity is ensured in the neighborhood of extraordinary vertices too. ■

N	λ_0	λ_1	λ_2	$\max_{i\geq 3} \lvert\lambda_i\rvert$
3	1.0000	0.4152	0.4152	0.2500
4	1.0000	0.5000	0.5000	0.2500
5	1.0000	0.5464	0.5464	0.3476
6	1.0000	0.5742	0.5742	0.4150
7	1.0000	0.5918	0.5918	0.4641
8	1.0000	0.6037	0.6037	0.5000
9	1.0000	0.6121	0.6121	0.5267

Table 2: The first 4 leading eigenvalues of the local subdivision matrix $\mathcal{A}$ of the subdivision scheme $\mathcal{S}_{\mathbf{a}_{1,\frac{1}{16}}}$.

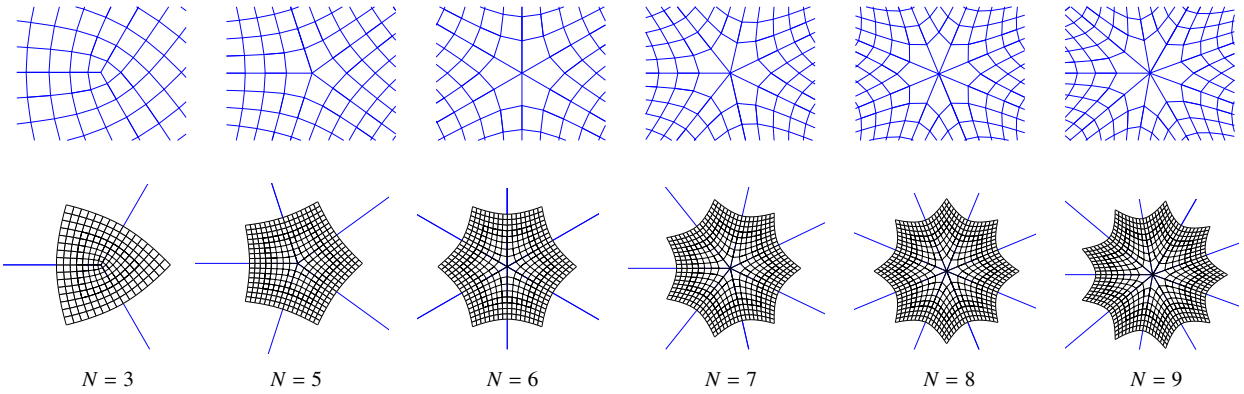

Figure 10: Visualization of characteristic meshes of the subdivision scheme $\mathcal{S}_{\mathbf{a}_{1,\frac{1}{16}}}$ for valences $N = 3, 5, 6, 7, 8, 9$ (first row) and corresponding characteristic maps in the neighborhood of the extraordinary vertex (second row) obtained from the above control nets after 4 rounds of subdivision.

Some examples of application of the subdivision scheme $\mathcal{S}_{\mathbf{a}_{1,\frac{1}{16}}}$ in case of quadrilateral meshes of arbitrary topology can be seen in Figure 11.

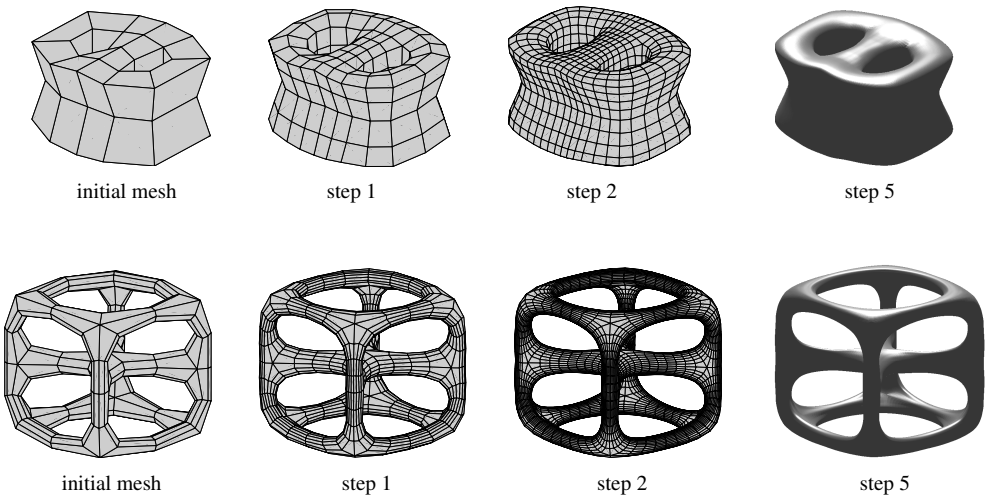

Figure 11: Surfaces obtained by applying 5 iterations of the interpolatory subdivision scheme $\mathcal{S}_{\mathbf{a}_{1,\frac{1}{16}}}$ to quadrilateral meshes of arbitrary topology.

5.2.1. Further inspections at extraordinary vertices: eigenanalysis depending on w and N

Since the smoothness analysis at extraordinary vertices was only established for $w = \frac{1}{16}$, we here investigate the behaviour of the first 4 leading eigenvalues of the local subdivision matrix $\mathcal{A}$ of the scheme $\mathcal{S}_{\mathbf{a}_{1,w}}$ in dependence of the free parameter w, in order to identify a certain range of values for which the subdivision scheme is potentially C^1 continuous when applied to arbitrary meshes with extraordinary vertices.
Denoting by λ_i, $i = 0, 1, ...$ the eigenvalues of the local subdivision matrix $\mathcal{A}$ ordered by modulus, we recall that for symmetric subdivision schemes $1 = \lambda_0 > \lambda_1 = \lambda_2 > |\lambda_3|$ is a necessary condition for C^1 continuity at extraordinary vertices. Therefore, aim of this subsection is to show that for w chosen in a certain range, the first 4 leading eigenvalues λ_i, $i = 0, ..., 3$ indeed respect the condition above. To this end we selected $w \in (0, \frac{1}{16}]$ (the case $w = 0$ is not considered because the scheme $\mathcal{S}_{\mathbf{a}_{1,0}}$ is already only C^0 in the regular case) and we plotted the curves describing the behaviour of these 4 eigenvalues. As we can see from Figure 12, it is always verified that $1 = \lambda_0$, $\lambda_1 = \lambda_2$ is a double real eigenvalue smaller than 1, and λ_3 is a real eigenvalue smaller than $\lambda_1 = \lambda_2$. In particular, although for values of w approaching to 0 the double eigenvalue λ_1 becomes closer and closer to the eigenvalue λ_3, for all tested valences N it always remains greater. Additionally, for increasing values of $N \geq 4$ we can observe that the distance between the subdominant double eigenvalue λ_1 and the sub-subdominant eigenvalue λ_3 becomes smaller and smaller at any fixed value of w. Anyway, for $N < 10$ it never vanishes. This trend is even better illustrated in Figure 13 where for some specific values of $w \in (0, \frac{1}{16}]$ we point out the behaviour of the first 4 leading eigenvalues in dependence of the valence N. As easily expected, the greater is the valence, the smaller is the distance between the subdominant and the sub-subdominant eigenvalue (see also Figure 14 where valences up to $N = 30$ have been considered).
From our analysis we can thus conclude that, for the interpolatory scheme $\mathcal{S}_{\mathbf{a}_{1,w}}$ with $w \in (0, \frac{1}{16}]$, the eigenvalues distribution is further and further away from the desired configuration and becomes potentially critical when the valence of the extraordinary vertex increases and the value of the parameter w approaches to 0.

6. A new non-tensor product dual approximating subdivision scheme with tension parameter

Applying the Refine-and-Smooth strategy illustrated in Section 4 with two smoothing stages, we obtain a dual approximating subdivision scheme for quadrilateral meshes. In the following we analyze the properties of such scheme both in the regular case ($N = 4$) and in correspondence of extraordinary faces of valence $N \neq 4$.

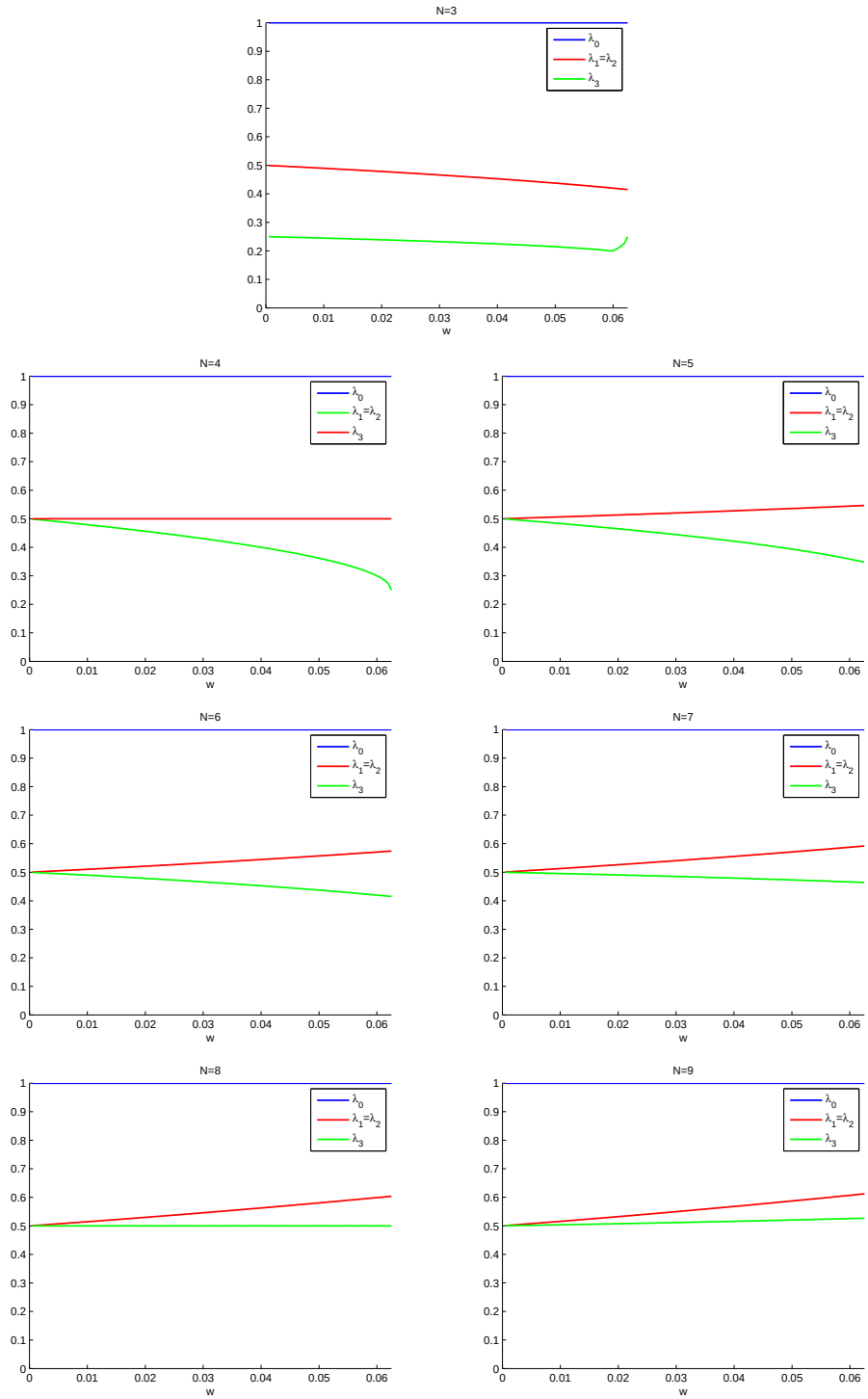

Figure 12: Behaviour of the first 4 leading eigenvalues of the local subdivision matrix $\mathcal{A}$ of the scheme $\mathcal{S}_{\mathbf{a}_{1,w}}$ for different values of the parameter $w \in (0, \frac{1}{16}]$ and valences $N < 10$. Note that the selected range of values for w is contained in $(0, \frac{2}{15})$ and thus, in the regular case $N = 4$, C^1 continuity is guaranteed in view of Proposition 5.1.

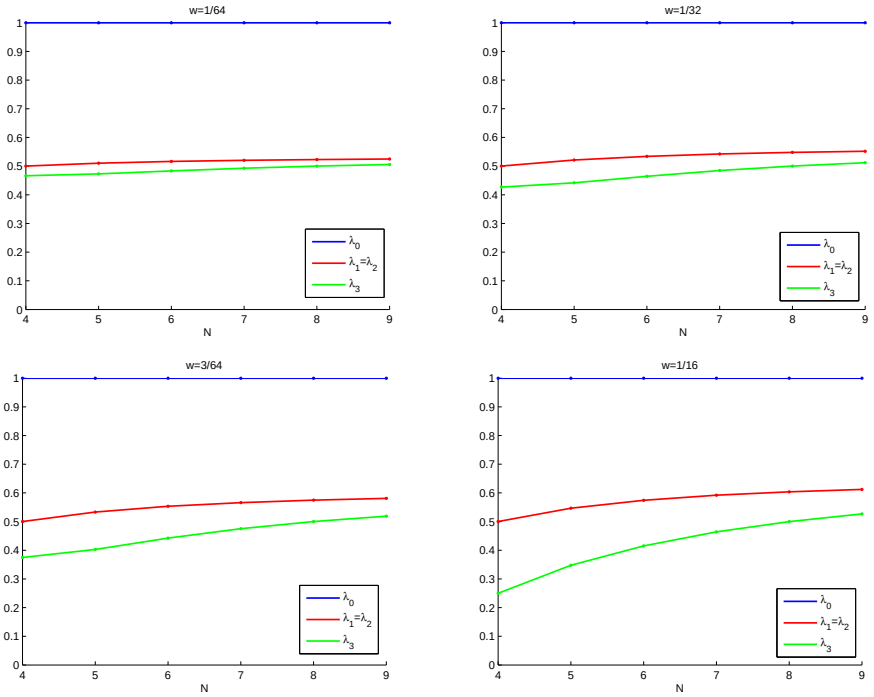

Figure 13: Behaviour of the first 4 leading eigenvalues of the local subdivision matrix $\mathcal{A}$ of the scheme $\mathcal{S}_{\mathbf{a}_{1,w}}$ for some specific values of the parameter $w \in (0, \frac{1}{16}]$ and for valences $N \leq 9$.

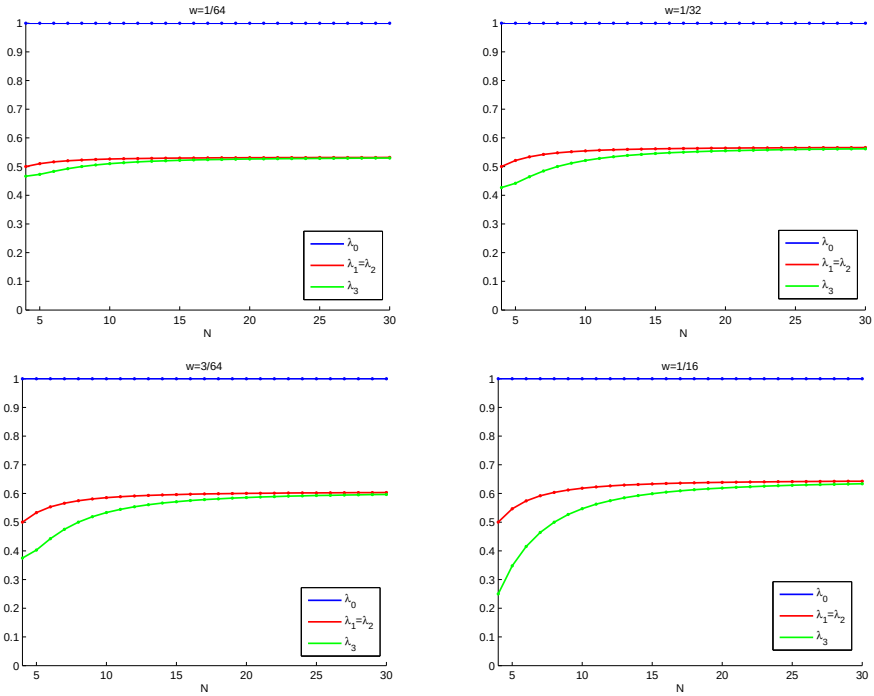

Figure 14: Behaviour of the first 4 leading eigenvalues of the local subdivision matrix $\mathcal{A}$ of the scheme $\mathcal{S}_{\mathbf{a}_{1,w}}$ for some specific values of the parameter $w \in (0, \frac{1}{16}]$ and for valences $N \leq 30$.

6.1. Properties of the regular case (N = 4)

When $N = 4$, the bivariate subdivision scheme $\mathcal{S}_{\mathbf{a}_{2,w}}$ has mask

$$\mathbf{a}_{2,w} = \begin{pmatrix} -\frac{5w}{256} & -\frac{15w}{256} & -\frac{45w}{256} & -\frac{95w}{256} & -\frac{95w}{256} & -\frac{45w}{256} & -\frac{15w}{256} & -\frac{5w}{256} \\ -\frac{15w}{256} & -\frac{33w}{256} & -\frac{59w}{256} & -\frac{117w}{256} & -\frac{117w}{256} & -\frac{59w}{256} & -\frac{33w}{256} & -\frac{15w}{256} \\ -\frac{45w}{256} & -\frac{59w}{256} & \frac{55w}{256}+\frac{1}{16} & \frac{145w}{256}+\frac{3}{16} & \frac{145w}{256}+\frac{3}{16} & \frac{55w}{256}+\frac{1}{16} & -\frac{59w}{256} & -\frac{45w}{256} \\ -\frac{95w}{256} & -\frac{117w}{256} & \frac{145w}{256}+\frac{3}{16} & \frac{355w}{256}+\frac{9}{16} & \frac{355w}{256}+\frac{9}{16} & \frac{145w}{256}+\frac{3}{16} & -\frac{117w}{256} & -\frac{95w}{256} \\ -\frac{95w}{256} & -\frac{117w}{256} & \frac{145w}{256}+\frac{3}{16} & \frac{355w}{256}+\frac{9}{16} & \frac{355w}{256}+\frac{9}{16} & \frac{145w}{256}+\frac{3}{16} & -\frac{117w}{256} & -\frac{95w}{256} \\ -\frac{45w}{256} & -\frac{59w}{256} & \frac{55w}{256}+\frac{1}{16} & \frac{145w}{256}+\frac{3}{16} & \frac{145w}{256}+\frac{3}{16} & \frac{55w}{256}+\frac{1}{16} & -\frac{59w}{256} & -\frac{45w}{256} \\ -\frac{15w}{256} & -\frac{33w}{256} & -\frac{59w}{256} & -\frac{117w}{256} & -\frac{117w}{256} & -\frac{59w}{256} & -\frac{33w}{256} & -\frac{15w}{256} \\ -\frac{5w}{256} & -\frac{15w}{256} & -\frac{45w}{256} & -\frac{95w}{256} & -\frac{95w}{256} & -\frac{45w}{256} & -\frac{15w}{256} & -\frac{5w}{256} \end{pmatrix}, \tag{6.1}$$

and symbol

$$\begin{aligned} a_{2,w}(z_1,z_2) &= \tfrac{1}{256}\, z_1^{-3} z_2^{-3}\,(1+z_1)^3(1+z_2)^3\Big(-5wz_1^4z_2^4 - 30wz_1^4z_2^2 - 5wz_1^4 \\ &+ 12wz_1^3z_2^3 + 40wz_1^3z_2^2 + 12wz_1^3z_2 - 30wz_1^2z_2^4 + 40wz_1^2z_2^3 + 4(4-17w)z_1^2z_2^2 \\ &+ 40wz_1^2z_2 - 30wz_1^2 + 12wz_1z_2^3 + 40wz_1z_2^2 + 12wz_1z_2 - 5wz_2^4 - 30wz_2^2 - 5w\Big). \end{aligned} \tag{6.2}$$

Since $a_{2,w}(z_1,z_2) = a_{2,w}(z_2,z_1)$, then $\mathcal{S}_{\mathbf{a}_{2,w}}$ is a scheme with symmetry relative to the two axes, but again it is a *non-tensor product* scheme. In fact $a_{2,w}(z_1,z_2)$ cannot be written as the product of a polynomial in z_1 with a polynomial in z_2. However, $a_{2,w}(z_1,1)$ coincides with the dual approximating 4-point scheme in [16], hence the bivariate scheme with symbol $a_{2,w}(z_1,z_2)$ can be interpreted as a non-tensor product extension of the dual approximating 4-point scheme with tension parameter (see Figure 15 for the plot of the corresponding basic limit function).

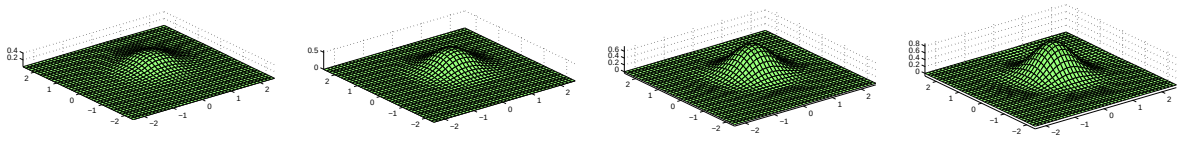

(a) $w = -\frac{1}{16}$ (b) $w = 0$ (c) $w = \frac{1}{16}$ (d) $w = \frac{1}{10}$

Figure 15: Basic limit function of $\mathcal{S}_{\mathbf{a}_{2,w}}$ for different values of w.

In the remaining part of this section we analyze the main properties fulfilled by this new dual approximating bivariate subdivision scheme when applied to a regular initial mesh.

In the following proposition we start by determining the parameter set Ω_2 for which the scheme $\mathcal{S}_{\mathbf{a}_{2,w}}$ turns out to be convergent, and we derive the subset of parameters corresponding to the generation of smooth limit surfaces. As done in the previous section, for this purpose we exploit the formalism of Laurent polynomials.

Proposition 6.1. *If $w \in (-\frac{24}{59}, \frac{8}{59})$ the subdivision scheme $\mathcal{S}_{\mathbf{a}_{2,w}}$ converges to a continuous surface when starting from any regular quadrilateral mesh. Moreover, if $w \in (-\frac{4}{13}, \frac{8}{75})$, then the obtained limit surface is C^1.*

Proof: Let us start by writing $a_{2,w}(z_1,z_2) = \left(\frac{1+z_1}{2}\right)^3 \left(\frac{1+z_2}{2}\right)^3 b_{2,w}(z_1,z_2)$ with

$$\begin{aligned} b_{2,w}(z_1,z_2) &= \tfrac{1}{4}\Big(-5wz_1^4z_2^4 - 30wz_1^4z_2^2 - 5wz_1^4 + 12wz_1^3z_2^3 + 40wz_1^3z_2^2 + 12wz_1^3z_2 - 30wz_1^2z_2^4 + 40wz_1^2z_2^3 \\ &+ 4(4-17w)z_1^2z_2^2 + 40wz_1^2z_2 - 30wz_1^2 + 12wz_1z_2^3 + 40wz_1z_2^2 + 12wz_1z_2 - 5wz_2^4 - 30wz_2^2 - 5w\Big). \end{aligned}$$

Since $a_{2,w}(z_1, z_2) = a_{2,w}(z_2, z_1)$, in view of [15, Theorem 4.30] we can determine the range of the parameter w which guarantees the convergence of the scheme $\mathcal{S}_{\mathbf{a}_{2,w}}$ by checking the contractivity of the scheme with symbol $\frac{1}{2}\left(\frac{1+z_1}{2}\right)^3\left(\frac{1+z_2}{2}\right)^2 b_{2,w}(z_1, z_2)$. This yields $w \in (-\frac{24}{59}, \frac{8}{59})$.
In the same spirit, the result on the C^1 continuity follows by checking the contractivity of the schemes with symbols $\frac{1}{2}\left(\frac{1+z_1}{2}\right)^3\left(\frac{1+z_2}{2}\right) b_{2,w}(z_1, z_2)$ and $\frac{1}{2}\left(\frac{1+z_1}{2}\right)^2\left(\frac{1+z_2}{2}\right)^2 b_{2,w}(z_1, z_2)$. ■

Indeed, when setting $w = \frac{1}{16}$, the limit surfaces produced by the subdivision scheme $\mathcal{S}_{\mathbf{a}_{2,w}}$ are even smoother, as shown in the following proposition.

Proposition 6.2. *The subdivision scheme $\mathcal{S}_{\mathbf{a}_{2,\frac{1}{16}}}$ produces C^2 limit surfaces when starting from any regular quadrilateral mesh.*

Proof: From the result in Proposition 6.1 we already know that the smoothness of the limit functions produced by the scheme is C^1. In order to show that when $w = \frac{1}{16}$ it is indeed C^2, exploiting the result in [15, Theorem 4.30], the proof consists in showing the contractivity of the symbols $\frac{1}{2}\left(\frac{1+z_1}{2}\right)^3 b_{2,w}(z_1, z_2)$ and $\frac{1}{2}\left(\frac{1+z_1}{2}\right)^2\left(\frac{1+z_2}{2}\right) b_{2,w}(z_1, z_2)$. ■

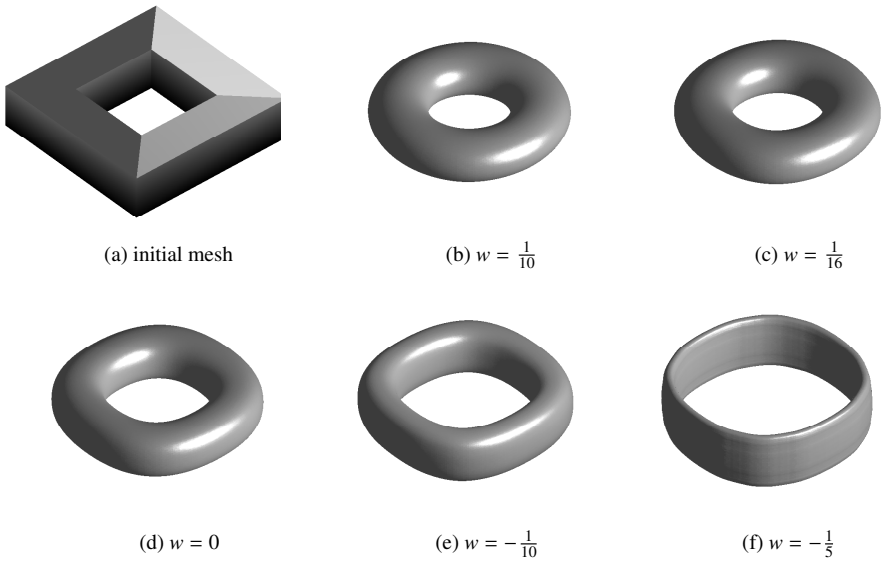

(a) initial mesh (b) $w = \frac{1}{10}$ (c) $w = \frac{1}{16}$

(d) $w = 0$ (e) $w = -\frac{1}{10}$ (f) $w = -\frac{1}{5}$

Figure 16: Surfaces obtained by applying 6 iterations of the dual approximating subdivision scheme $\mathcal{S}_{\mathbf{a}_{2,w}}$ to the regular mesh in (a) for different choices of the tension parameter.

In Figure 16 we illustrate the effect of the tension parameter w for values in the above determined range $(-\frac{4}{13}, \frac{8}{75})$.
In the following two propositions we investigate the capability of the subdivision scheme $\mathcal{S}_{\mathbf{a}_{2,w}}$, with $w \in \Omega_2 = (-\frac{24}{59}, \frac{8}{59})$, of generating and reproducing polynomials.

Proposition 6.3. *The subdivision scheme $\mathcal{S}_{\mathbf{a}_{2,w}}$ generates Π_2^2 for all $w \in \Omega_2$ and generates Π_4^2 for $w = \frac{1}{16}$.*

The detailed proof of Proposition 6.3 is given in Appendix A.

Remark 9. *It is interesting to observe that, since the subdivision scheme $\mathcal{S}_{\mathbf{a}_{2,\frac{1}{16}}}$ generates Π_4^2, then in view of the results in [5], the symbol $z_1^3 z_2^3\, a_{2,\frac{1}{16}}(z_1, z_2)$ can be decomposed as*

$$z_1^3 z_2^3\, a_{2,\frac{1}{16}}(z_1, z_2) = 4 \sum_{B_{i,j,k} \in I_5} L_{i,j,k}\, \sigma_{i,j,k}(z_1, z_2)\, B_{i,j,k}(z_1, z_2),$$

where

- $B_{i,j,k}(z_1, z_2) = \left(\frac{1+z_1}{2}\right)^i \left(\frac{1+z_2}{2}\right)^j \left(\frac{1+z_1 z_2}{2}\right)^k$, *$i, j, k \in \mathbb{N}_0$ are normalized mask symbols of three-directional box-splines;*
- $I_5 = \{B_{5,5,0}, B_{5,0,5}, B_{0,5,5}, B_{4,4,1}, B_{4,1,4}, B_{1,4,4}, B_{3,3,2}, B_{3,2,3}, B_{2,3,3}\}$ *is the set of generators of* $\mathcal{I}^5 = \{p \in \Pi^2 : (D^{(j_1,j_2)}p)(\mathbf{u}) = 0$ *for* $\mathbf{u} \in \{(1,-1), (-1,1), (-1,-1)\}, j_1 + j_2 < 5\}$*;*
- $\sigma_{i,j,k}(z_1, z_2)$ *are Laurent polynomials normalized by* $\sigma_{i,j,k}(1,1) = 1$*;*
- $L_{i,j,k}$ *are real coefficients that fulfill the condition* $\sum L_{i,j,k} = 1$.

More precisely, a representation of the symbol $z_1^3 z_2^3\, a_{2,\frac{1}{16}}(z_1, z_2)$ *in terms of three-directional box-splines from the list* I_5 *is given by*

$$z_1^3 z_2^3\, a_{2,\frac{1}{16}}(z_1, z_2) = 4\Big(L_{5,5,0}\,\sigma_{5,5,0}(z_1, z_2)\,B_{5,5,0}(z_1, z_2) + L_{4,4,1}\,\sigma_{4,4,1}(z_1, z_2)\,B_{4,4,1}(z_1, z_2) + L_{3,3,2}\,\sigma_{3,3,2}(z_1, z_2)\,B_{3,3,2}(z_1, z_2)\Big),$$

with

$$L_{5,5,0} = \frac{\theta_1(\theta_2 + 72)}{(\theta_1 + \theta_2)(\theta_2 - 36)}, \qquad L_{4,4,1} = \frac{\theta_2(\theta_2 + 72)}{(\theta_1 + \theta_2)(\theta_2 - 36)}, \qquad L_{3,3,2} = -\frac{108}{\theta_2 - 36},$$

and the normalized symbols

$$\begin{aligned}
\sigma_{5,5,0}(z_1, z_2) &= \tfrac{1}{16\theta_1(\theta_2+72)}\Big((\theta_1 + \theta_2)(\theta_3 - 4(7\theta_2 - 468))z_1^2 z_2^2 - 5(\theta_1 + \theta_2)(\theta_2 - 36)(z_1^2 + z_2^2)\\
&- 2(540\theta_1 + 828\theta_2 - 27\theta_1\theta_2 - 23\theta_2^2)z_1 z_2 - (576\theta_2 + \theta_1\theta_3 + \theta_2\theta_3 + 8\theta_2^2)\Big),\\
\sigma_{4,4,1}(z_1, z_2) &= \tfrac{1}{16\theta_2(\theta_2+72)}\Big((\theta_1 + \theta_2)(4(7\theta_2 - 468) - \theta_3)z_1^2 z_2^2 + 5(\theta_1 + \theta_2)(\theta_2 - 36)(z_1^2 + z_2^2)\\
&+ (360\theta_1 + 648\theta_2 - 22\theta_1\theta_2 - \theta_1\theta_3 - \theta_2\theta_3 - 18\theta_2^2)z_1 z_2\\
&+ (936\theta_1 + 1224\theta_2 - 14\theta_1\theta_2 + \theta_1\theta_3 + \theta_2\theta_3 - 10\theta_2^2)(z_1 + z_2) + 4\theta_2(3\theta_1 + 4\theta_2 + 72)\Big),\\
\sigma_{3,3,2}(z_1, z_2) &= \tfrac{1}{6912}\Big((33\theta_2 - \theta_3 - 2052)z_1^2 z_2^2 + (7\theta_2 + \theta_3 + 612)(z_1^2 + z_2^2) - 4(17\theta_2 - 1044)z_1 z_2\\
&- 4(\theta_2 - 468)(z_1 + z_2) + (29\theta_2 - \theta_3 - 180)\Big),
\end{aligned}$$

expressed in terms of the arbitrary coefficients $\theta_1, \theta_2, \theta_3 \in \mathbb{R}$. *Since the generators* $B_{5,5,0}(z_1, z_2)$, $B_{4,4,1}(z_1, z_2)$ *and* $B_{3,3,2}(z_1, z_2)$ *are all multiples of* $B_{3,3,0}(z_1, z_2)$*, there follows that the symbol* $z_1^3 z_2^3\, a_{2,\frac{1}{16}}(z_1, z_2)$ *contains the factor* $(1 + z_1)^3(1 + z_2)^3$*, as can be noticed from equation* (6.2).

Proposition 6.4. *If applying the parameter shift* $(\tau_1, \tau_2) = \left(\frac{1}{2}, \frac{1}{2}\right)$*, the subdivision scheme* $\mathcal{S}_{\mathbf{a}_{2,w}}$ *reproduces* Π_1^2 *for all* $w \in \Omega_2$ *and reproduces* Π_3^2 *for* $w = \frac{1}{16}$*, with respect to the dual parametrization in* (2.1).

The reader may find the full proof of Proposition 6.4 in Appendix A.

We conclude by observing that, in view of Proposition 6.2, the subdivision scheme $\mathcal{S}_{\mathbf{a}_{2,\frac{1}{16}}}$ has the same smoothness properties of the bi-cubic B-spline surface, but, instead of being a tensor product primal scheme, it is a non-tensor product dual scheme. Moreover, in view of Proposition 6.4 it is featured by the capability of reproducing Π_3^2, instead of simply having linear precision, and thus the approximation order of the new scheme is higher than the one of the bi-cubic B-spline surface. Although the approximation order derived from the reproduction degree is usually not optimal since, after suitably preprocessing the initial data, an approximation order of one larger than the generation degree can be achieved [20], considering that the new scheme is able to generate Π_4^2 whereas the bi-cubic B-spline scheme only Π_3^2, even when applying the preprocessing, the approximation order of the new scheme turns out to be higher. This means that the limit surface of the new scheme approximates the initial data better than the bi-cubic B-spline scheme (see, e.g, Figure 17).

6.2. Properties of the irregular case

We start by highlighting a property of the subdivision scheme $\mathcal{S}_{\mathbf{a}_{2,w}}$ when $w = 0$. In the regular regions, since $a_{2,0}(z_1, z_2) = \frac{1}{16} z_1^{-1} z_2^{-1} (1 + z_1)^3(1 + z_2)^3$, it is clear that the dual approximating subdivision scheme $\mathcal{S}_{\mathbf{a}_{2,0}}$ reduces to the tensor product of the quadratic B-spline scheme, i.e., to the regular case of Doo-Sabin's scheme (see Figure 15(b)).

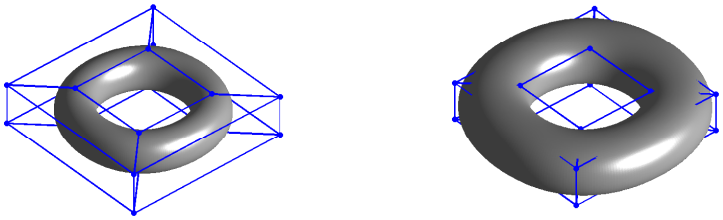

Figure 17: Comparison between a bi-cubic B-spline surface (left) and the limit surface obtained by the new approximating scheme $\mathcal{S}_{\mathbf{a}_{2,\frac{1}{16}}}$ (right) when applied to the same regular mesh.

Analogously, in correspondence to extraordinary faces with N edges, the scheme reduces to the Catmull-Clark variant of Doo-Sabin's algorithm (see [2]), which consists in using the weights

$$v_{i,j} = \begin{cases} \frac{1}{2} + \frac{1}{4N}, & \text{if } j = i; \\ \frac{1}{8} + \frac{1}{4N}, & \text{if } |j - i| = 1; \\ \frac{1}{4N}, & \text{otherwise} \end{cases}$$

in equation (4.2) to compute the new vertices inside the extraordinary face. Such scheme is known to produce C^1 limit surfaces for any arbitrary initial mesh [12], and the 4 leading eigenvalues of its local subdivision matrix $\mathcal{A}$ for valences $N \leq 9$ are the ones in Table 3 (see also [12, Table 3]).

N	λ_0	λ_1	λ_2	$\max_{i\geq 3} \lvert\lambda_i\rvert$
3	1.0000	0.3750	0.3750	0.2500
4	1.0000	0.5000	0.5000	0.2500
5	1.0000	0.5773	0.5773	0.2977
6	1.0000	0.6250	0.6250	0.3750
7	1.0000	0.6559	0.6559	0.4444
8	1.0000	0.6768	0.6768	0.5000
9	1.0000	0.6915	0.6915	0.5434

Table 3: The first 4 leading eigenvalues of the local subdivision matrix $\mathcal{A}$ of the subdivision scheme $\mathcal{S}_{\mathbf{a}_{2,0}}$.

In the following we continue by analyzing the smoothness properties of the subdivision scheme $\mathcal{S}_{\mathbf{a}_{2,\frac{1}{16}}}$ when applied to arbitrary meshes, since again the parameter value $w = \frac{1}{16}$ is the one that provides the smoothest surfaces in the regular regions.

Proposition 6.5. *The subdivision scheme $\mathcal{S}_{\mathbf{a}_{2,\frac{1}{16}}}$ produces limit surfaces that are C^2-continuous everywhere except in the neighborhood of extraordinary vertices of valence $N < 10$ where they are only C^1.*

Proof: We start by observing that, in case the initial mesh contains some extraordinary vertices, then after the first subdivision step an extraordinary face with N edges is created in correspondence to an extraordinary vertex of valence N. The number of extraordinary faces generated by the scheme after the first iteration remains the same during all the subdivision process and each extraordinary face becomes isolated in an otherwise regular tiling of the surface. Thus, we can analyze the smoothness properties of the scheme $\mathcal{S}_{\mathbf{a}_{2,\frac{1}{16}}}$ following the same reasoning in the proof of Proposition 5.4. More precisely, after recalling that C^2 smoothness of the limit surface in regular regions has been already established in Proposition 6.2, we proceed by computing the eigenvalues of the local subdivision matrix $\mathcal{A}$ defined in the neighborhood of an extraordinary face of valence $3 \leq N \leq 9$. As shown in Table 4, the leading eigenvalue of $\mathcal{A}$

(corresponding to the dominant eigenvalue of the Fourier block $\hat{\mathcal{A}}_0^{(N)}$) is $\lambda_0 = 1$, whereas the subdominant eigenvalue of $\mathcal{A}$ is given by $\lambda_1 = \lambda_2 < 1$, where λ_1 is the dominant eigenvalue of $\hat{\mathcal{A}}_1^{(N)}$ and λ_2 that of $\hat{\mathcal{A}}_{N-1}^{(N)}$. Since the moduli of all remaining eigenvalues of $\mathcal{A}$ are strictly smaller than λ_2, and the characteristic maps defined in the neighborhood of the centroids of the extraordinary faces turn out to be both regular (i.e. have non-zero Jacobian determinant everywhere) and injective (as illustrated by the pictures of Figure 18), C^1-continuity at irregular regions is proved for all $N < 10$. ■

N	λ_0	λ_1	λ_2	$\max_{i\geq 3} \lvert\lambda_i\rvert$
3	1.0000	0.4077	0.4077	0.2500
4	1.0000	0.5000	0.5000	0.2500
5	1.0000	0.5480	0.5480	0.3317
6	1.0000	0.5744	0.5744	0.3958
7	1.0000	0.5901	0.5901	0.4417
8	1.0000	0.6001	0.6001	0.4735
9	1.0000	0.6069	0.6069	0.4956

Table 4: The first 4 leading eigenvalues of the local subdivision matrix $\mathcal{A}$ of the subdivision scheme $\mathcal{S}_{\mathbf{a}_{2,\frac{1}{16}}}$.

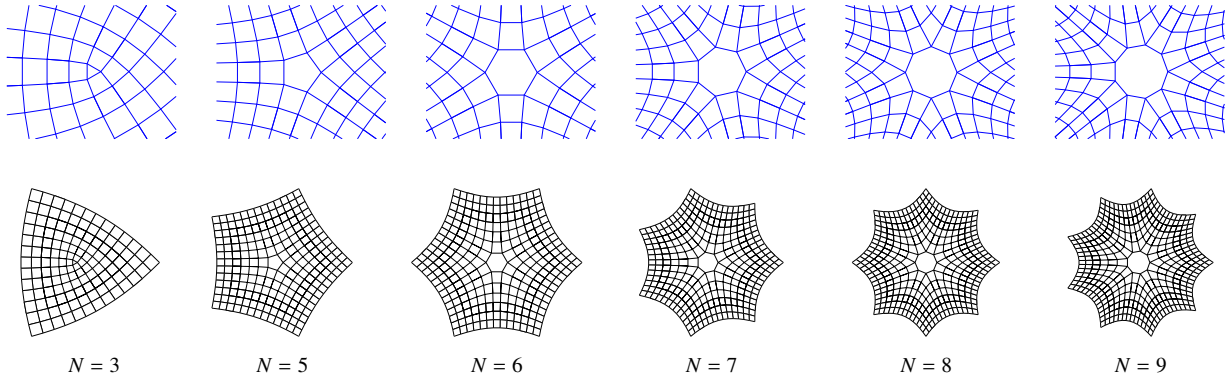

Figure 18: Visualization of characteristic meshes of the subdivision scheme $\mathcal{S}_{\mathbf{a}_{2,\frac{1}{16}}}$ for valences $N = 3, 5, 6, 7, 8, 9$ (first row) and corresponding characteristic maps in the neighborhood of the centroid of the extraordinary face (second row) obtained after 4 rounds of subdivision.

In Figure 19 we show the limit surfaces obtained by applying the subdivision scheme $\mathcal{S}_{\mathbf{a}_{2,\frac{1}{16}}}$ to quadrilateral meshes of arbitrary topology.

6.2.1. Further inspections at extraordinary vertices: eigenanalysis depending on w and N

Following the reasoning in Subsection 5.2.1, we again intend to investigate the fulfillment of the necessary conditions for C^1 continuity regarding the first 4 leading eigenvalues λ_i, $i = 0, ..., 3$ of the local subdivision matrix $\mathcal{A}$ (ordered by modulus), when the free parameter w is chosen in the neighborhood of $\frac{1}{16}$. In other words, aim of this subsection is to show that for $w \in (0, \frac{1}{10}]$ (the case $w = 0$ is not considered here since already investigated in [12]), the first 4 leading eigenvalues λ_i, $i = 0, ..., 3$ are real eigenvalues that indeed respect the condition $1 = \lambda_0 > \lambda_1 = \lambda_2 > \lambda_3$. As we can see from Figure 20, the cases $N = 3$ and $N > 4$ behave in opposite ways. In fact, in the first case, for increasing values of w the double real eigenvalue λ_1 stays farther and farther from the real eigenvalue λ_3; in contrast, in the second case, the greater the value of w, the closer are the values of λ_1 and λ_3. Additionally, as also previously observed for the interpolatory subdivision scheme $\mathcal{S}_{\mathbf{a}_{1,w}}$, for increasing values of $N > 4$ the distance between the subdominant double eigenvalue λ_1 and the sub-subdominant eigenvalue λ_3 progressively reduces. This trend is again

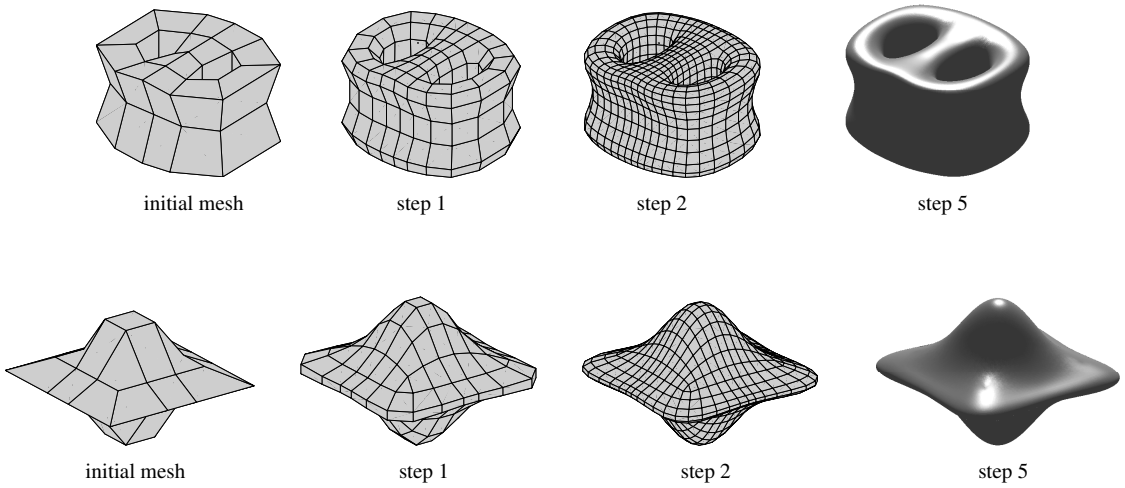

Figure 19: Surfaces obtained by applying 5 iterations of the dual approximating subdivision scheme $\mathcal{S}_{\mathbf{a}_{2,\frac{1}{16}}}$ to quadrilateral meshes of arbitrary topology.

more evident if, for a fixed value of w, we plot the behaviour of the first 4 leading eigenvalues in dependence of the valence N (see Figure 21). Although for valencies $N \leq 9$ the two curves are always well separated, increasing the value of N they become closer and closer, so confirming the fact that high valencies are the most critical to smoothness analysis. But, differently from the interpolatory scheme $\mathcal{S}_{\mathbf{a}_{1,w}}$, here the largest values of w are the ones that yield less separated eigenvalues in case of high valencies.

7. Conclusions

In this paper we presented a new constructive approach to design tension-controlled univariate and bivariate families of alternating primal/dual subdivision schemes in a unified framework. The approach is based on a Refine-and-Smooth subdivision algorithm that originates from a parameter-dependent variant of the Lane-Riesenfeld algorithm. The first two family members obtained in the univariate case are two well-known schemes with tension parameter, proposed in the literature via isolated constructions. Differently, the first two family members obtained in the bivariate case are an interpolatory and a dual approximating scheme for quadrilateral meshes with arbitrary topology never investigated before. In particular, the member corresponding to the choice $n = 1$ has been shown to be a non-tensor product extension of the interpolatory 4-point scheme with tension parameter [14], whereas the one corresponding to the choice $n = 2$ an analogous extension of the dual approximating 4-point scheme [16]. The tuning of the tension parameter to maximize the degree of polynomial reproduction, provided in the univariate case a revisitation of the family of Hormann-Sabin's schemes with cubic precision [18], whereas in the bivariate case the proposal of a novel family of non-tensor product subdivision schemes with bivariate cubic precision.

Acknowledgements
The author would like to thank Giorgio Clauser for cooperating in producing several pictures contained in this paper. Many thanks also go to the anonymous referees for their careful reading of the manuscript and for their useful suggestions which helped to improve the presentation of the results.

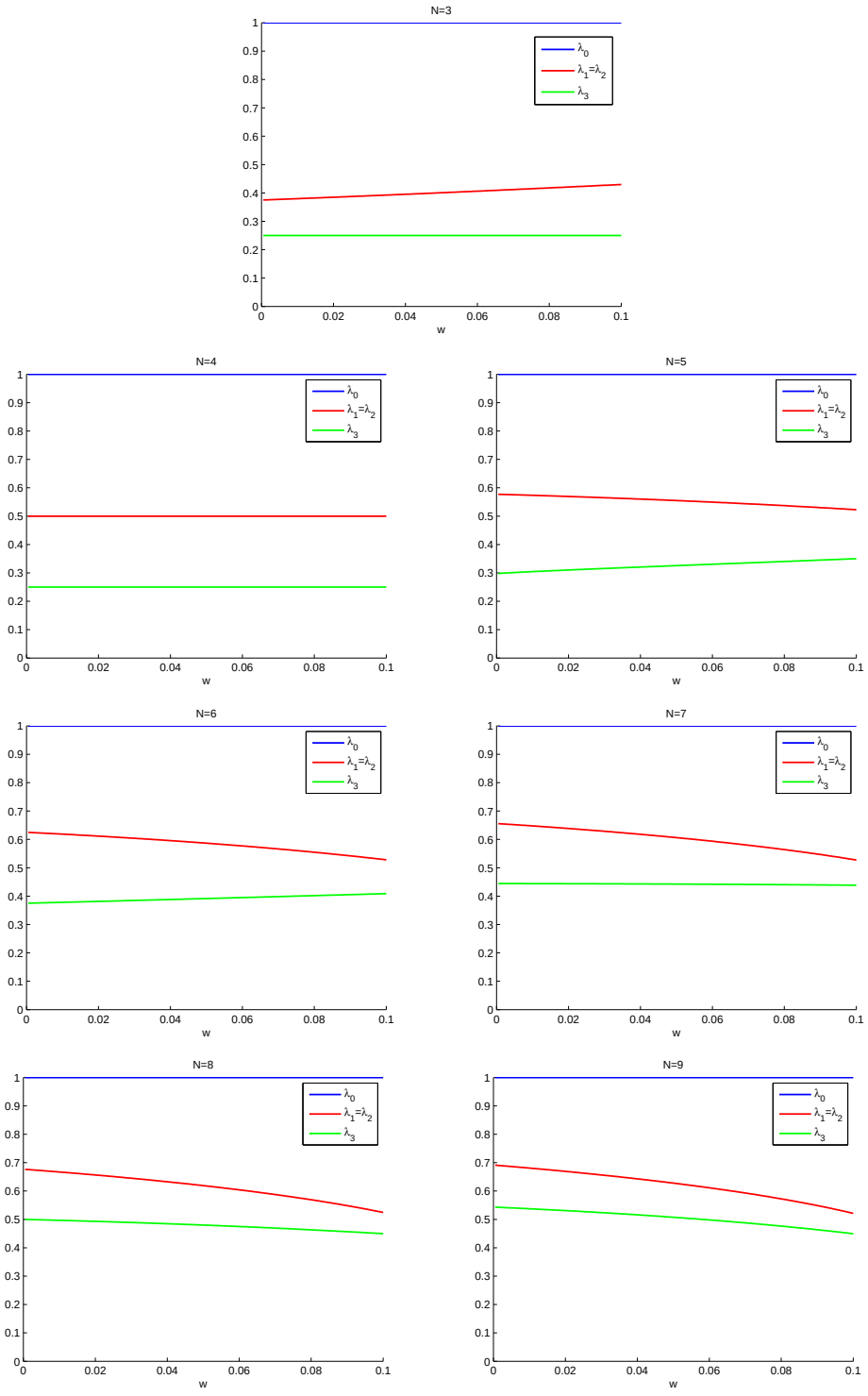

Figure 20: Behaviour of the first 4 leading eigenvalues of the local subdivision matrix $\mathcal{A}$ of the scheme $\mathcal{S}_{\mathbf{a}_{2,w}}$ for different values of the parameter $w \in (0, \frac{1}{10}]$ and valences $N < 10$. Note that the selected range of values for w is contained in $(-\frac{4}{13}, \frac{8}{75})$ and thus, in the regular case $N = 4$, C^1 continuity is guaranteed in view of Proposition 6.1.

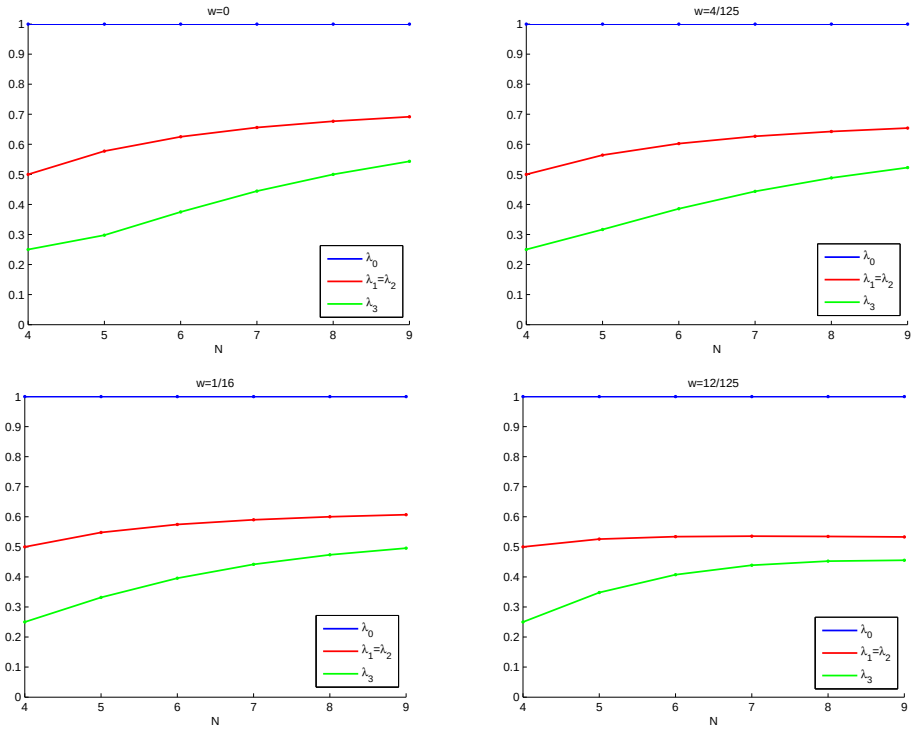

Figure 21: Behaviour of the first 4 leading eigenvalues of the local subdivision matrix $\mathcal{A}$ of the scheme $\mathcal{S}_{\mathbf{a}_{2,w}}$ for some specific values of the parameter $w \in (0, \frac{1}{10}]$ and for valences $N \leq 9$.

Appendix A.

Appendix A.1. Proof of Proposition 5.2

Let $\mathbf{u}_1 = (1,-1)$, $\mathbf{u}_2 = (-1,1)$, $\mathbf{u}_3 = (-1,-1)$ and let $D^{\mathbf{j}}$, with $\mathbf{j} \in \mathbb{N}_0^2$, denote a directional derivative. Since the conditions

$$
\begin{aligned}
& a_{1,w}(1,1) = 4, \\
& a_{1,w}(\mathbf{u}_1) = a_{1,w}(\mathbf{u}_2) = a_{1,w}(\mathbf{u}_3) = 0, \\
& D^{(1,0)}a_{1,w}(\mathbf{u}_1) = D^{(1,0)}a_{1,w}(\mathbf{u}_2) = D^{(1,0)}a_{1,w}(\mathbf{u}_3) = 0, \\
& D^{(0,1)}a_{1,w}(\mathbf{u}_1) = D^{(0,1)}a_{1,w}(\mathbf{u}_2) = D^{(0,1)}a_{1,w}(\mathbf{u}_3) = 0, \\
& D^{(2,0)}a_{1,w}(\mathbf{u}_1) = D^{(2,0)}a_{1,w}(\mathbf{u}_3) = 0, \quad D^{(2,0)}a_{1,w}(\mathbf{u}_2) = 2(16w-1), \\
& D^{(1,1)}a_{1,w}(\mathbf{u}_1) = D^{(1,1)}a_{1,w}(\mathbf{u}_2) = D^{(1,1)}a_{1,w}(\mathbf{u}_3) = 0, \\
& D^{(0,2)}a_{1,w}(\mathbf{u}_1) = 2(16w-1), \quad D^{(0,2)}a_{1,w}(\mathbf{u}_2) = D^{(0,2)}a_{1,w}(\mathbf{u}_3) = 0, \\
& D^{(3,0)}a_{1,w}(\mathbf{u}_1) = D^{(3,0)}a_{1,w}(\mathbf{u}_3) = 0, \quad D^{(3,0)}a_{1,w}(\mathbf{u}_2) = 6(16w-1), \\
& D^{(2,1)}a_{1,w}(\mathbf{u}_1) = D^{(2,1)}a_{1,w}(\mathbf{u}_2) = D^{(2,1)}a_{1,w}(\mathbf{u}_3) = 0, \\
& D^{(1,2)}a_{1,w}(\mathbf{u}_1) = D^{(1,2)}a_{1,w}(\mathbf{u}_2) = D^{(1,2)}a_{1,w}(\mathbf{u}_3) = 0, \\
& D^{(0,3)}a_{1,w}(\mathbf{u}_1) = 6(16w-1), \quad D^{(0,3)}a_{1,w}(\mathbf{u}_2) = D^{(0,3)}a_{1,w}(\mathbf{u}_3) = 0,
\end{aligned}
\tag{A.1}
$$

are satisfied by the symbol $a_{1,w}(z_1, z_2)$ in (5.2), recalling the result in Proposition 2.2 - case (i) the claim is proved. ■

Appendix A.2. Proof of Proposition 5.3

Let $D^{\mathbf{j}}$, with $\mathbf{j} \in \mathbb{N}_0^2$, denote a directional derivative. Since the symbol $a_{1,w}(z_1, z_2)$ in (5.2) satisfies the conditions

$$
\begin{aligned}
&D^{(1,0)}a_{1,w}(1,1) = D^{(0,1)}a_{1,w}(1,1) = 0,\\
&D^{(1,1)}a_{1,w}(1,1) = 0, \quad D^{(2,0)}a_{1,w}(1,1) = D^{(0,2)}a_{1,w}(1,1) = 2(1-16w),\\
&D^{(2,1)}a_{1,w}(1,1) = D^{(1,2)}a_{1,w}(1,1) = 0, \quad D^{(3,0)}a_{1,w}(1,1) = D^{(0,3)}a_{1,w}(1,1) = 6(16w-1),
\end{aligned}
$$

together with the ones given in (A.1), in view of Proposition 2.2 -case (*ii*), the claim is proved. ■

Appendix A.3. Proof of Proposition 6.3

Let $\mathbf{u}_1 = (1,-1)$, $\mathbf{u}_2 = (-1,1)$ and $\mathbf{u}_3 = (-1,-1)$. Since the conditions

$$
\begin{aligned}
&a_{2,w}(\mathbf{u}_1) = a_{2,w}(\mathbf{u}_2) = a_{2,w}(\mathbf{u}_3) = 0,\\
&D^{(1,0)}a_{2,w}(\mathbf{u}_1) = D^{(1,0)}a_{2,w}(\mathbf{u}_2) = D^{(1,0)}a_{2,w}(\mathbf{u}_3) = 0,\\
&D^{(0,1)}a_{2,w}(\mathbf{u}_1) = D^{(0,1)}a_{2,w}(\mathbf{u}_2) = D^{(0,1)}a_{2,w}(\mathbf{u}_3) = 0,\\
&D^{(2,0)}a_{2,w}(\mathbf{u}_1) = D^{(2,0)}a_{2,w}(\mathbf{u}_2) = D^{(2,0)}a_{2,w}(\mathbf{u}_3) = 0,\\
&D^{(1,1)}a_{2,w}(\mathbf{u}_1) = D^{(1,1)}a_{2,w}(\mathbf{u}_2) = D^{(1,1)}a_{2,w}(\mathbf{u}_3) = 0,\\
&D^{(0,2)}a_{2,w}(\mathbf{u}_1) = D^{(0,2)}a_{2,w}(\mathbf{u}_2) = D^{(0,2)}a_{2,w}(\mathbf{u}_3) = 0,\\
&D^{(3,0)}a_{2,w}(\mathbf{u}_1) = D^{(3,0)}a_{2,w}(\mathbf{u}_3) = 0, \quad D^{(3,0)}a_{2,w}(\mathbf{u}_2) = 3(16w-1),\\
&D^{(2,1)}a_{2,w}(\mathbf{u}_1) = D^{(2,1)}a_{2,w}(\mathbf{u}_2) = D^{(2,1)}a_{2,w}(\mathbf{u}_3) = 0,\\
&D^{(1,2)}a_{2,w}(\mathbf{u}_1) = D^{(1,2)}a_{2,w}(\mathbf{u}_2) = D^{(1,2)}a_{2,w}(\mathbf{u}_3) = 0,\\
&D^{(0,3)}a_{2,w}(\mathbf{u}_1) = 3(16w-1), \quad D^{(0,3)}a_{2,w}(\mathbf{u}_2) = D^{(0,3)}a_{2,w}(\mathbf{u}_3) = 0,\\
&D^{(4,0)}a_{2,w}(\mathbf{u}_1) = D^{(4,0)}a_{2,w}(\mathbf{u}_3) = 0, \quad D^{(4,0)}a_{2,w}(\mathbf{u}_2) = 12(16w-1),\\
&D^{(3,1)}a_{2,w}(\mathbf{u}_1) = D^{(3,1)}a_{2,w}(\mathbf{u}_3) = 0, \quad D^{(3,1)}a_{2,w}(\mathbf{u}_2) = 3\left(8w-\tfrac{1}{2}\right),\\
&D^{(2,2)}a_{2,w}(\mathbf{u}_1) = D^{(2,2)}a_{2,w}(\mathbf{u}_2) = D^{(2,2)}a_{2,w}(\mathbf{u}_3) = 0,\\
&D^{(1,3)}a_{2,w}(\mathbf{u}_1) = 3\left(8w-\tfrac{1}{2}\right), \quad D^{(1,3)}a_{2,w}(\mathbf{u}_2) = D^{(1,3)}a_{2,w}(\mathbf{u}_3) = 0,\\
&D^{(0,4)}a_{2,w}(\mathbf{u}_1) = 12(16w-1), \quad D^{(0,4)}a_{2,w}(\mathbf{u}_2) = D^{(0,4)}a_{2,w}(\mathbf{u}_3) = 0,
\end{aligned}
\tag{A.2}
$$

are verified by the symbol $a_{2,w}(z_1, z_2)$ in (6.2), recalling the results in Proposition 2.2 - case (*i*) the claim is proved. ■

Appendix A.4. Proof of Proposition 6.4

Since the conditions

$$
\begin{aligned}
&a_{2,w}(1,1) = 4,\\
&D^{(1,0)}a_{2,w}(1,1) - 4\tau_1 = D^{(0,1)}a_{2,w}(1,1) - 4\tau_2 = 0,\\
&D^{(1,1)}a_{2,w}(1,1) - 4\tau_1\tau_2 = 0,\\
&D^{(2,0)}a_{2,w}(1,1) - 4\tau_1(\tau_1-1) = D^{(0,2)}a_{2,w}(1,1) - 4\tau_2(\tau_2-1) = 3(1-16w),\\
&D^{(2,1)}a_{2,w}(1,1) - 4\tau_1(\tau_1-1)\tau_2 = D^{(1,2)}a_{2,w}(1,1) - 4\tau_1\tau_2(\tau_2-1) = 3\left(\tfrac{1}{2}-8w\right),\\
&D^{(3,0)}a_{2,w}(1,1) - 4\tau_1(\tau_1-1)(\tau_1-2) = D^{(0,3)}a_{2,w}(1,1) - 4\tau_2(\tau_2-1)(\tau_2-2) = 9\left(8w-\tfrac{1}{2}\right),
\end{aligned}
$$

are satisfied by the symbol $a_{2,w}(z_1, z_2)$ in (6.2) together with the ones given in (A.2), in view of Proposition 2.2 - case (*ii*) the claim is proved. ■

References

[1] T.J. Cashman, K. Hormann, U. Reif, Generalized Lane–Riesenfeld algorithms, Comput. Aided Geom. Design 30 (2013), 398–409.

[2] E. Catmull, J. Clark, Recursively generated B-spline surfaces on arbitrary topological meshes, Computer Aided Design 10 (1978), 350–355.

[3] G.M. Chaikin, An algorithm for high speed curve generation, Computer Graphics and Image Processing, 3(4) (1974), 346–349.

[4] M. Charina, C. Conti, Polynomial reproduction of multivariate scalar subdivision schemes, J. Comput. Applied Math., 240 (2013), 51–61.

[5] M. Charina, C. Conti, K. Jetter, G. Zimmermann, Scalar multivariate subdivision schemes and box splines, Comput. Aided Geom. Design 28 (2011), 285–306.

[6] M. Charina, C. Conti, L. Romani, Reproduction of exponential polynomials by multivariate non-stationary subdivision schemes with a general dilation matrix, Numer. Math. 127(2) (2014), 223–254.

[7] C. Conti, K. Hormann, Polynomial reproduction for univariate subdivision schemes of any arity, J. Approx. Theory, 163 (2011), 413–437.

[8] C. Conti, L. Romani, Algebraic conditions on non-stationary subdivision symbols for exponential polynomial reproduction, J. Comput. Applied Math., 236(4) (2011), 543–556.

[9] C. Conti, L. Romani, Dual univariate m-ary subdivision schemes of de Rham-type, J. Math. Anal. Appl. 407 (2013), 443–456.

[10] C. Deng, W. Ma, Constructing an interpolatory subdivision scheme from Doo-Sabin subdivision, 12th Intern. Conf. on Computer-Aided Design and Computer Graphics (2011), 215–222.

[11] G. Deslauriers, S. Dubuc, Symmetric iterative interpolation processes. Constr. Approx. 5 (1989), 49–68.

[12] D. Doo, M. Sabin, Analysis of the behaviour of recursive division surfaces near extraordinary points. Computer Aided Design 10(6) (1978), 356–360.

[13] N. Dyn, K. Hormann, M.A. Sabin, Z. Shen, Polynomial reproduction by symmetric subdivision schemes, J. Approx. Theory 155 (2008), 28–42.

[14] N. Dyn, D. Levin, J.A. Gregory, A 4-point interpolatory subdivision scheme for curve design, Comput. Aided Geom. Design 4 (1987), 257–268.

[15] N. Dyn, D. Levin, Subdivision schemes in geometric modelling, Acta Numer. 11 (2002), 73–144.

[16] N. Dyn, M. Floater and K. Hormann, A C^2 four-point subdivision scheme with fourth-order accuracy and its extensions. In: M. Dæhlen, K. Mørken, L.L. Schumaker (Eds.), Mathematical Methods for Curves and Surfaces: Tromsø 2004, 145–156, Nashboro Press (2005).

[17] M. Floater, G. Muntingh, Exact regularity of pseudo-splines. arXiv/1209.2692, 2012.

[18] K. Hormann, M.A. Sabin, A family of subdivision schemes with cubic precision, Comput. Aided Geom. Design 25 (2008), 41–52.

[19] J.M. Lane, R.F. Riesenfeld, A theoretical development for the computer generation and display of piecewise polynomial surfaces, IEEE Transactions on Pattern Analysis and Machine Intelligence 2(1) (1980), 35–46.

[20] A. Levin, Polynomial generation and quasi-interpolation in stationary non-uniform subdivision, Comput. Aided Geom. Design, 20 (2003), 41–60.

[21] H. Prautzsch, Q. Chen, Analyzing midpoint subdivision, Comput. Aided Geom. Design 28 (2011), 407–419.

[22] U. Reif, A unified approach to subdivision algorithms near extraordinary vertices, Comput. Aided Geom. Design 12 (1995), 153–174.

[23] J. Stam, On subdivision schemes generalizing uniform B-spline surfaces of arbitrary degree, Comput. Aided Geom. Design 18 (2001), 383–396.

[24] D. Zorin, P. Schröder, A unified framework for primal/dual quadrilateral subdivision schemes, Comput. Aided Geom. Design 18 (2001), 429–454.